とが考えられる．そして，RAナース細胞により維持された破骨細胞前駆細胞は，周囲に存在する骨芽細胞やT細胞での産生が亢進しているRANKL刺激により破骨細胞に分化し骨破壊を起こしていると考えている（**図4**）[14]．

おわりに

RAにおける骨粗鬆症について，とくに傍関節性骨粗鬆症における臨床病態についてわれわれの知見をもとに述べた．昨今生物学的製剤の登場でRA治療体系が大きく変わろうとしている．しかし，現時点ではRAの治癒は困難であり，骨破壊の進行を遅らせることは可能と予想されるが，完全に防止することは困難である．われわれは，M-CSFを阻害することによりRAによる骨破壊を抑制できる可能性を報告した[15]．今後，炎症を強力に抑制するとともに，骨破壊を抑制する治療法開発が重要と考える．

文献

1) Tak PP and Bresnihan B. The pathogenesis and prevention of joint damage in rheumatoid arthritis: advances from synovial biopsy and tissue analysis. *Arthritis Rheum* 2000, 43(12): 2619-2633.
2) Teitelbaum SL. Bone resorption by osteoclasts. *Science* 2000, 289(5484): 1504-1508.
3) Suda T, Takahashi N, Udagawa N, *et al.* Modulation of osteoclast differentiation and function by the new members of the tumor necrosis factor receptor and ligand families. *Endocr Rev* 1999, 20(3): 345-357.
4) Gravallese EM, Manning C, Tsay A, *et al.* Synovial tissue in rheumatoid arthritis is a source of osteoclast differentiation factor. *Arthritis Rheum* 2000, 43(2): 250-258.
5) Takayanagi H, Iizuka H, Juji T, *et al.* Involvement of receptor activator of nuclear factor kappaB ligand/osteoclast differentiation factor in osteoclastogenesis from synoviocytes in rheumatoid arthritis. *Arthritis Rheum* 2000, 43(2): 259-269.
6) Shigeyama Y, Pap T, Kunzler P, *et al.* Expression of osteoclast differentiation factor in rheumatoid arthritis. *Arthritis Rheum* 2000, 43(11): 2523-2530.
7) Takeuchi E, Tomita T, Toyosaki-Maeda T, *et al.* Establishment and characterization of nurse cell-like stromal cell lines from synovial tissues of patients with rheumatoid arthritis. *Arthritis Rheum* 1999, 42(2): 221-228.
8) Tomita T, Takeuchi E, Toyosaki-Maeda T, *et al.* Establishment of nurse-like stromal cells from bone marrow of patients with rheumatoid arthritis: indication of characteristic bone marrow microenvironment in patients with rheumatoid arthritis. *Rheumatology* (Oxford) 1999, 38(9): 854-863.
9) Wekerle H and Ketelsen UP. Thymic nurse cells—Ia-bearing epithelium involved in T-lymphocyte differentiation? *Nature* 1980, 283(5745): 402-404.
10) Nicholson GC, Malakellis M, Collier FM, *et al.* Induction of osteoclasts from CD14-positive human peripheral blood mononuclear cells by receptor activator of nuclear factor kappaB ligand (RANKL). *Clin Sci* (Lond) 2000, 99(2): 133-140.
11) Matsuzaki K, Katayama K, Takahashi Y, *et al.* Human osteoclast-like cells are formed from peripheral blood mononuclear cells in a coculture with SaOS-2 cells transfected with the parathyroid hormone (PTH)/PTH-related protein receptor gene. *Endocrinology* 1999, 140(2): 925-932.
12) Itoh K, Udagawa N, Matsuzaki K, *et al.* Importance of membrane- or matrix-associated forms of M-CSF and RANKL/ODF in osteoclastogenesis supported by SaOS-4/3 cells expressing recombinant PTH/PTHrP receptors. *J Bone Miner Res* 2000, 15(9): 1766-1775.
13) Toyosaki-Maeda T, Takano H, Tomita T, *et al.* Differentiation of monocytes into multinucleated giant bone-resorbing cells: two-step differentiation induced by nurse-like cells and cytokines. *Arthritis Res* 2001, 3(5): 306-310.
14) Tsuboi H, Udagawa N, Hashimoto J, *et al.* Nurse-like cells from patients with rheumatoid arthritis support survival of osteoclast precursors via macrophage-colony stimulating factor production. *Arthritis Rheum* 2005, 52(12): 3819-3828.
15) Ando W, Hashimoto J, Nampei A, *et al.* Imatinib mesylate inhibits osteoclastogenesis and joint destruction in rats with collagen-induced arthritis (CIA). *J Bone Miner Met* 2006. (in press)

Vol 443|26 October 2006|doi:10.1038/nature05245

LETTERS

Chronic polyarthritis caused by mammalian DNA that escapes from degradation in macrophages

Kohki Kawane[1,3,4], Mayumi Ohtani[1,4], Keiko Miwa[1,4]†, Takuji Kizawa[2], Yoshiyuki Kanbara[5], Yoshichika Yoshioka[5], Hideki Yoshikawa[2] & Shigekazu Nagata[1,3,4]

A large amount of chromosomal DNA is degraded during programmed cell death and definitive erythropoiesis[1]. DNase II is an enzyme that digests the chromosomal DNA of apoptotic cells and nuclei expelled from erythroid precursor cells after macrophages have engulfed them[1,2]. Here we show that *DNase II*$^{-/-}$*IFN-IR*$^{-/-}$ mice and mice with an induced deletion of the *DNase II* gene develop a chronic polyarthritis resembling human rheumatoid arthritis. A set of cytokine genes was strongly activated in the affected joints of these mice, and their serum contained high levels of anti-cyclic citrullinated peptide antibody, rheumatoid factor and matrix metalloproteinase-3. Early in the pathogenesis, expression of the gene encoding tumour necrosis factor (TNF)-α was upregulated in the bone marrow, and administration of anti-TNF-α antibody prevented the development of arthritis. These results indicate that if macrophages cannot degrade mammalian DNA from erythroid precursors and apoptotic cells, they produce TNF-α, which activates synovial cells to produce various cytokines, leading to the development of chronic polyarthritis.

DNase II$^{-/-}$ mice die as embryos as a result of the constitutive production of interferon (IFN)-β[3,4], and this lethality can be rescued by a deficiency of the *IFN-IR* gene[5]. *DNase II*$^{-/-}$*IFN-IR*$^{-/-}$ mice were born normal, at a slightly reduced mendelian ratio, but they developed polyarthritis as they aged (see below). To examine whether mice carrying a single deletion in *DNase II* gene develop arthritis, we introduced a floxed allele into the *DNase II* gene (Supplementary Fig. S1). These mice were crossed with *Mx1-Cre* mice, which carry the *Cre* gene under the control of *Mx1*, an IFN-inducible promoter[6], and *DNase II*$^{flox/-}$*Mx1-Cre*^{T} mice were established. When these mice were treated with poly(I)•poly(C) to induce IFN, the floxed region of *DNase II* gene was deleted within 2 months in the spleen (Supplementary Fig. S2), and DNase II messenger RNA was undetectable in the spleen and bone marrow (Supplementary Fig. S3). Hereafter we refer to the poly(I)•poly(C)-treated *DNase II*$^{flox/-}$ mice as *DNase II*$^{\Delta/-}$ mice.

The inactivation of the *DNase II* gene in adult mice was not lethal. However, *DNase II*$^{\Delta/-}$, but not poly(I)•poly(C)-treated

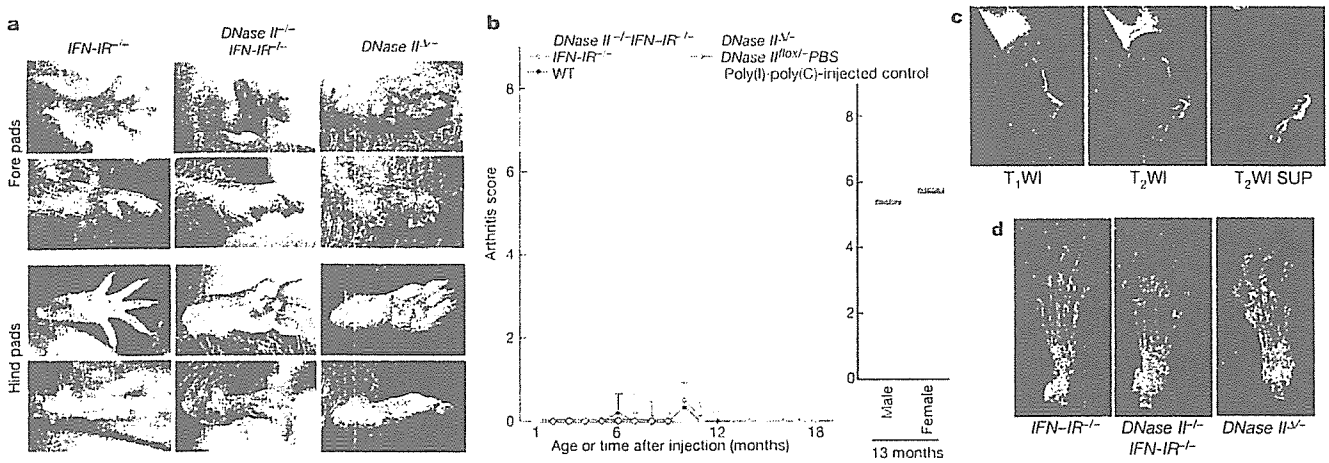

Figure 1 | Arthritis in *DNase II*$^{-/-}$*IFN-IR*$^{-/-}$ and *DNase II*$^{\Delta/-}$ mice. **a**, Joint swelling of *DNase II*$^{-/-}$*IFN-IR*$^{-/-}$ at the age of 12.5 months, and *DNase II*$^{\Delta/-}$ 8–10 months after treatment with poly(I)•poly(C). Joints of *IFN-IR*$^{-/-}$ mice are shown as control. **b**, Left, joints of wild-type (n = 3–4), *IFN-IR*$^{-/-}$ (n = 5–8) and *DNase II*$^{-/-}$*IFN-IR*$^{-/-}$ (n = 9–10) mice were examined at the indicated ages. *DNase II*$^{flox/-}$ (n = 8–10) and *DNase II*$^{flox/-}$ (n = 11–15) littermates were given poly(I)•poly(C) or PBS (n = 5), and examined after the indicated periods. The arthritis scores are plotted as means and s.d. Right, the scores of 13-month-old *DNase II*$^{-/-}$*IFN-IR*$^{-/-}$ are plotted according to sex. The average values are indicated by horizontal red lines. **c**, MRI of the hindlimb of a 15-month-old *DNase II*$^{-/-}$*IFN-IR*$^{-/-}$ mouse. T_1-weighted images (T_1WI), T_2-weighted images (T_2WI) and T_2-weighted images with fat suppression (T_2WI SUP) are shown. **d**, Radiographic examination of the hindlimbs from a 15.5-month-old *DNase II*$^{-/-}$*IFN-IR*$^{-/-}$ and a *DNase II*$^{\Delta/-}$ mouse 10 months after treatment with poly(I)•poly(C).

[1]Department of Genetics and [2]Department of Orthopaedics, Osaka University Medical School, Osaka 565-0871, Japan. [3]Laboratory of Genetics, Integrated Biology Laboratories, Graduate School of Frontier Biosciences, Osaka University, Osaka 565-0871, Japan. [4]Solution Oriented Research for Science and Technology, Japan Science and Technology Corporation, Osaka 565-0871, Japan. [5]High Field Magnetic Resonance Imaging Research Institute, Advanced Medical Science Research Centre, Iwate Medical University, Takizawa 020-0173, Japan. †Present address: Laboratory of Cell Lineage Modulation, RIKEN Kobe Institute, Kobe 650-0047, Japan.

DNase II$^{flox/+}$ mice, developed chronic polyarthritis in a time-dependent manner (Fig. 1). In *DNase II*$^{-/-}$*IFN-IR*$^{-/-}$ mice at 2–3 months of age or in *DNase II*$^{flox/-}$ mice 2–3 months after treatment with poly(I)•poly(C), forelimbs and hindlimbs began to swell. Swelling affected first the digit, then the foot, and finally the wrist and ankles. Individual mutant mice followed a significantly different time course, but all the mice were eventually affected. As swelling progressed, the mutant mice gradually lost their grasp strength, and their joints became deformed. There was no clear difference between male and female mice in disease development (Fig. 1b). Magnetic resonance imaging (MRI) of the affected joints showed high-intensity signals on the T_2-weighted image around tarsal bones and phalanges (Fig. 1c). These high-intensity regions were also observed on the fat-suppressed T_2-weighted image, indicating that the joints suffered massive inflammation. Radiographic examination revealed destruction, erosion, and deformity of the subchondral bones (Fig. 1d).

Histology of the swollen joints from both *DNase II*$^{-/-}$*IFN-IR*$^{-/-}$ and *DNase II*$^{A/-}$ mice showed severe synovitis with villus proliferation accompanied by pannus formation (Fig. 2a). Pannus filled the joint cavity, eroded cartilage, destroyed bones, and occasionally penetrated the bone marrow. Pannus was dominated by macrophages carrying the CD68 antigen, among which tartrate-resistant acid phosphatase (TRAP)-positive osteoclasts were at the leading edge. Infiltration of subsynovial tissues by T cells and neutrophils was also observed (Fig. 2a, and data not shown). The abnormal inflammation was limited to the joints, and no apparent disorder was found in the skin, liver, salivary glands, gut or blood vessels of most of the mice.

A set of cytokines and chemokines is known to be highly expressed in the joints of human patients with rheumatoid arthritis[7–9]. Real-time polymerase chain reaction (PCR) analysis indicated that levels of mRNA for TNF-α, interleukin (IL)-1β, IL-6, IL-10, IFN-β and IFN-γ in the affected joints of *DNase II*$^{-/-}$*IFN-IR*$^{-/-}$ and *DNase II*$^{A/-}$ mice were 5–100-fold those in control mice (Fig. 2b). The level of mRNA for IL-18 in the joints of *DNase II*$^{-/-}$ mice was comparable to that in control mice. However, the level of IL-18 protein was very high in the serum of *DNase II*$^{-/-}$*IFN-IR*$^{-/-}$ and *DNase II*$^{A/-}$ mice (Fig. 2c), indicating that the expression of IL-18 might be regulated post-transcriptionally. Matrix metalloproteinase (MMP)-3 is produced by synovial cells of human patients with rheumatoid arthritis and seems to be involved in the degradation of the extracellular matrix[10]. Accordingly, the level of the mRNA for MMP-3 in the joints of *DNase II*$^{-/-}$*IFN-IR*$^{-/-}$ and *DNase II*$^{A/-}$ mice was more than 25-fold that in control mice (Fig. 2b), and its protein level in the serum was also 2–3-fold higher in the mutant mice (Fig. 2c). Anti-cyclic citrullinated peptide (CCP) antibody,

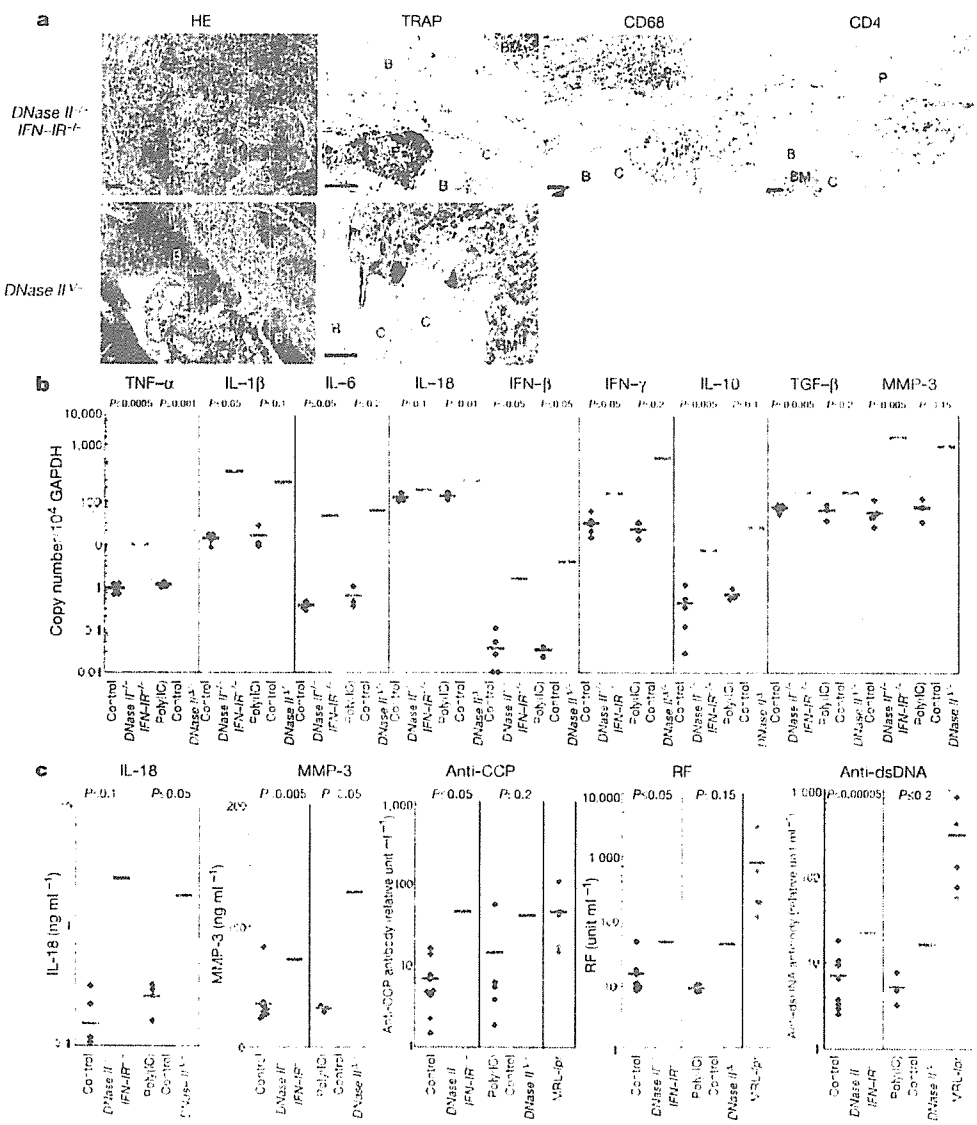

Figure 2 | Inflammatory arthritis in *DNase II*$^{-/-}$*IFN-IR*$^{-/-}$ mice. **a**, Joint sections from 8–16.5-month-old *DNase II*$^{-/-}$*IFN-IR*$^{-/-}$ or *DNase II*$^{flox/-}$ mice 10 months after treatment with poly(I)•poly(C) were stained with haematoxylin/eosin (HE), TRAP, anti-CD68 and anti-CD4. P, pannus; B, bone; C, cartilage; BM, bone marrow. Scale bar, 50 μm. **b**, RNAs were prepared from the joints of 7.5–13.5-month-old control or *DNase II*$^{-/-}$*IFN-IR*$^{-/-}$, and those of poly(I)•poly(C)-treated *DNase II*$^{flox/+}$ (poly(IC) control) or *DNase II*$^{A/-}$ mice. The mRNA levels for the indicated cytokines quantified by real-time PCR are expressed relative to mRNA for glyceraldehyde-3-phosphate dehydrogenase (GAPDH). **c**, The concentrations of IL-18, MMP-3, anti-CCP, rheumatoid factor (RF) and anti-dsDNA in the sera from 7.5–16.5-month-old control or *DNase II*$^{-/-}$*IFN-IR*$^{-/-}$, and from poly(I)•poly(C)-treated *DNase II*$^{flox/+}$ or *DNase II*$^{A/-}$ mice are shown. Some parameters were determined for 3–7.5 month-old MRL-*lpr* mice. In **b** and **c**, horizontal red lines indicate the average values. Welch's *t*-test was used to test for difference, and *P* values are shown.

which is specifically observed in human patients with rheumatoid arthritis[11], and rheumatoid factor were also detected at high levels in the serum of *DNase II*$^{-/-}$*IFN-IR*$^{-/-}$ and *DNase II*$^{+/-}$ mice (Fig. 2c). The level of anti-double-stranded DNA (dsDNA) antibody in *DNase II*$^{-/-}$*IFN-IR*$^{-/-}$ mice was about threefold that in wild-type mice, but this value was less than one-tenth of that observed in *lpr* mice, which develop an autoimmune disease similar to systemic lupus erythematosus[12].

DNase II$^{-/-}$*IFN-IR*$^{-/-}$ and *DNase II*$^{+/-}$ mice were slightly anaemic (hematocrit 40–45) and had clear growth retardation (data not shown). They developed splenomegaly from the age of 1 month, which became prominent as the mice aged; the weight of the spleen of 7.5–16.5-month-old *DNase II*$^{-/-}$*IFN-IR*$^{-/-}$ mice was about fivefold that of control mice (Fig. 3a). Splenomegaly was due to enlargement of the red pulp. We and others have reported previously that fetal liver and thymus of *DNase II*$^{-/-}$ mice contain many abnormal macrophages carrying undigested DNA from erythroid precursor cells or apoptotic cells[3,4,13]. Similarly, numerous abnormal macrophages carrying DNA in lysosomes were found in bone marrow, spleen and other tissues of the adult *DNase II*$^{-/-}$*IFN-IR*$^{-/-}$ and *DNase II*$^{+/-}$ mice (Fig. 3b). In addition, the serum of 4–6-week-old *DNase II*$^{-/-}$*IFN-IR*$^{-/-}$ mice contained about 10 μg ml^{-1} DNA, and this level decreased as the mice aged (Fig. 3c). *DNase II*$^{+/-}$ mice also carried a low but significant level of DNA in their serum. It is likely that the undigested DNA leaked from the macrophages into the bloodstream.

Cytokines can affect the pathogenesis of human rheumatoid arthritis[5]; we therefore examined the involvement of cytokines in our model. In comparison with that of control mice (less than 20 pg ml^{-1}), the serum concentration of TNF-α in *DNase II*$^{-/-}$*IFN-IR*$^{-/-}$ mice was higher (about 100 pg ml^{-1}) at 4–6 weeks of age (Fig. 3d), before the joints showed any apparent abnormality. A similar high concentration of TNF-α was observed in *DNase II*$^{+/-}$ mice. In contrast, other cytokines, such as IL-6, IL-1β, IFN-γ, granulocyte/macrophage colony-stimulating factor and IL-4 were undetectable in the serum of *DNase II* mutant mice. We previously reported that the fetal liver of *DNase II*$^{-/-}$ embryos constitutively expresses various cytokines[14]. Real-time PCR indicated that the level of mRNA for TNF-α in the bone marrow of 1-month-old *DNase II*$^{-/-}$*IFN-IR*$^{-/-}$ mice was twice that the level in age-matched control mice (Fig. 3e).

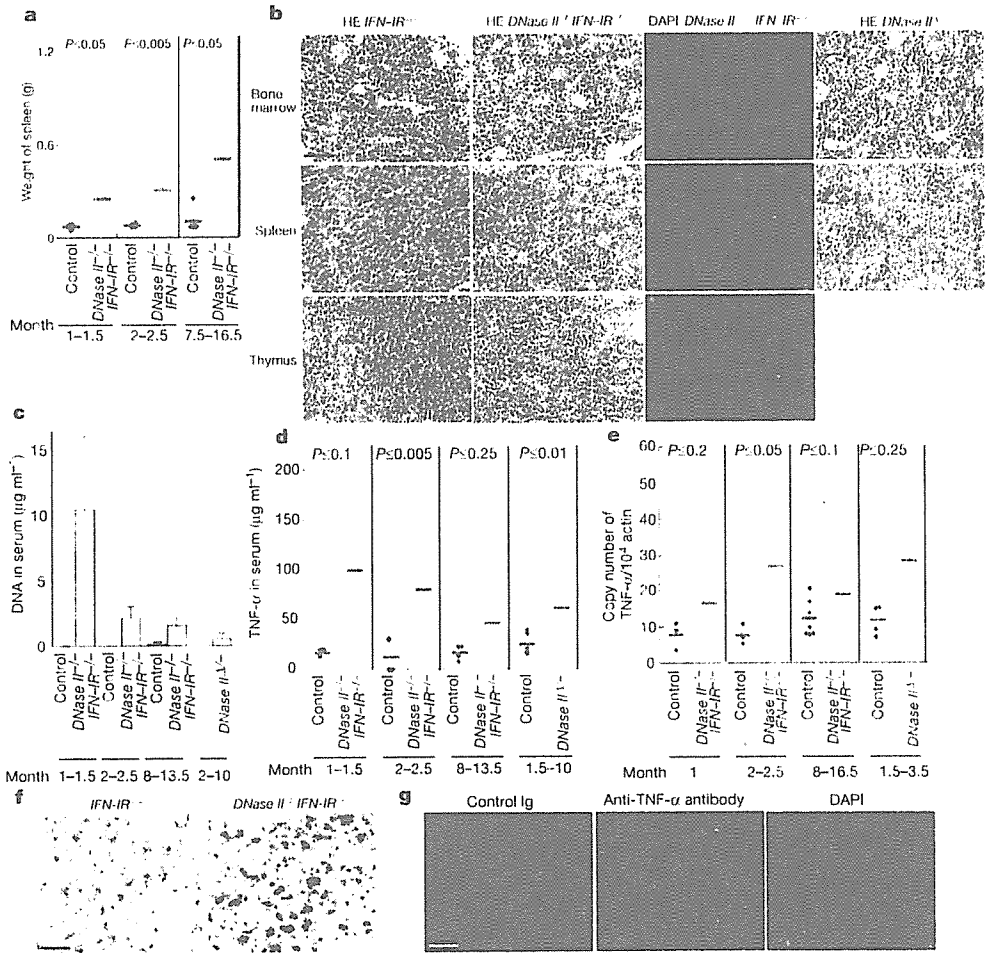

Figure 3 | Abnormal macrophages. **a**, The weight of spleens from control and *DNase II*$^{-/-}$*IFN-IR*$^{-/-}$ (four to seven mice) at the indicated ages. **b**, Bone marrow, spleen and thymus of 4–8-week-old *IFN-IR*$^{-/-}$ and *DNase II*$^{-/-}$*IFN-IR*$^{-/-}$ and *DNase II*$^{+/-}$ mice 10 months after treatment with poly(I)•poly(C) were stained with haematoxylin/eosin stain (HE) or 4′,6-diamidino-2-phenylindole (DAPI). Scale bar, 50 μm. **c**, DNA concentration in the serum of control, *DNase II*$^{-/-}$*IFN-IR*$^{-/-}$ and *DNase II*$^{+/-}$ mice (two to six animals for each) at the indicated ages. Results are plotted as means and s.d. **d**, Serum TNF-α concentration of control and *DNase II*$^{-/-}$*IFN-IR*$^{-/-}$, and *DNase II*$^{+/-}$ and *DNase II*$^{flox/-}$ littermates after treatment with poly(I)•poly(C) (three to six mice for each). **e**, mRNA for TNF-α in the bone marrow of control and *DNase II*$^{-/-}$*IFN-IR*$^{-/-}$, and that of poly(I)•poly(C)-treated *DNase II*$^{+/-}$ and *DNase II*$^{flox/-}$ littermates, quantified by real-time PCR, expressed relative to mRNA for β-actin. **f**, Bone marrow from 2-month-old *IFN-IR*$^{-/-}$ and *DNase II*$^{-/-}$*IFN-IR*$^{-/-}$ mice were stained with anti-CD68. Scale bar, 50 μm. **g**, Bone marrow from 1.5-month-old *DNase II*$^{-/-}$*IFN-IR*$^{-/-}$ mice were stained with goat normal IgG or anti-mouse TNF-α. The DAPI staining profile is also shown. Scale bar, 50 μm. In **a**, **d** and **e**, horizontal red lines indicate the average values. Welch's *t*-test was used to test for difference, and *P* values are shown.

The level of mRNA for TNF-α had increased further in these mutant mice by the age of 2–2.5 months, when definitive erythropoiesis is still active. A similar high level of mRNA for TNF-α was found in the bone marrow of *DNase II*$^{d/-}$ mice. Immunohistochemical analyses of the bone marrow (Fig. 3f) showed that the number of macrophages carrying the CD68 antigen in *DNase II*$^{-/-}$*IFN-IR*$^{-/-}$ mice did not differ significantly from that in control mice. However, CD68 was more intensely labelled in *DNase II*$^{-/-}$*IFN-IR*$^{-/-}$ mice, indicating that the macrophages carrying undigested DNA might have been activated[15]. Accordingly, TNF-α was detected in the cells carrying DNA (Fig. 3g).

To determine the effect of blocking TNF-α during the induction of arthritis, 4-week-old *DNase II*$^{-/-}$*IFN-IR*$^{-/-}$ or *DNase II*$^{+/-}$*IFN-IR*$^{-/-}$ littermates were given the neutralizing anti-TNF-α twice a week. *DNase II*$^{-/-}$*IFN-IR*$^{-/-}$ mice that received phosphate-buffered saline (PBS) started to develop arthritis when they were 8–14 weeks old (Fig. 4a). Accordingly, the serum MMP-3 level increased significantly (Fig. 4b). In contrast, mice treated with anti-TNF-α did not develop arthritis at this age, and their serum MMP-3 level was comparable to or slightly higher than that of *DNase II*$^{+/-}$*IFN-IR*$^{-/-}$ control mice. The expression of mRNA for TNF-α, IL-1β, IL-6 and MMP-3 at the joints was also blocked by the anti-TNF-α (Fig. 4c).

We then examined the therapeutic effect of anti-TNF-α after *DNase II*$^{-/-}$*IFN-IR*$^{-/-}$ mice had developed arthritis. Four *DNase II*$^{-/-}$*IFN-IR*$^{-/-}$ mice that showed an arthritis clinical score of 2.5–6 were treated twice a week with anti-TNF-α, and the serum MMP-3 level, which decreases with anti-TNF-α therapy in humans[16], was monitored. As shown in Fig. 4d, after 3 weeks of treatment the serum MMP-3 level had decreased to about one-third of its level before treatment. A decrease in the clinical score of the joints was apparent in two mice. The foot joints were then removed from all the mice, and the cytokine mRNA levels were determined. The joints of *DNase II*$^{-/-}$*IFN-IR*$^{-/-}$ mice receiving PBS carried 5–30-fold the levels of mRNA for TNF-α, IL-6, IL-1β and MMP-3 than those of *DNase II*$^{+/-}$*IFN-IR*$^{-/-}$ control mice, but the mRNA levels in the joints of *DNase II*$^{-/-}$*IFN-IR*$^{-/-}$ mice treated with anti-TNF-α were significantly decreased (Fig. 4e).

Systemic expression of TNF-α in a transgenic mouse model causes the development of chronic polyarthritis, indicating that TNF-α can trigger the disease[17]. Moreover, human patients with rheumatoid arthritis respond well to anti-TNF-α therapy[18,19]. However, the cause of the *TNF-α* gene expression in patients has not been established. We showed that macrophages carrying undigested DNA produce TNF-α, and that anti-TNF-α efficiently blocked the development of polyarthritis in *DNase II*-null mice. It is likely that TNF-α produced by *DNase II*$^{-/-}$ macrophages triggered the pathogenesis by stimulating the growth of synovial cells and by activating cytokine genes in synovial tissues. More than 10^{10} red blood cells are generated in the human body every day, and the same number of nuclei are expelled from erythroid precursor cells and degraded by DNase II in bone marrow macrophages. The DNA of apoptotic cells, of which 10^{8}–10^{9} are generated every day, is degraded by DNase II in macrophages. Our results indicate that a failure in this process can lead to the development of polyarthritis. Monocyte activation early in the onset of human rheumatoid arthritis has been noticed in some patients[20]; this is consistent with our results and indicates that the activation of macrophages could be an initiator of the pathogenic cascade in human arthritis. In addition to anti-TNF-α therapy, human patients with rheumatoid arthritis respond to treatment

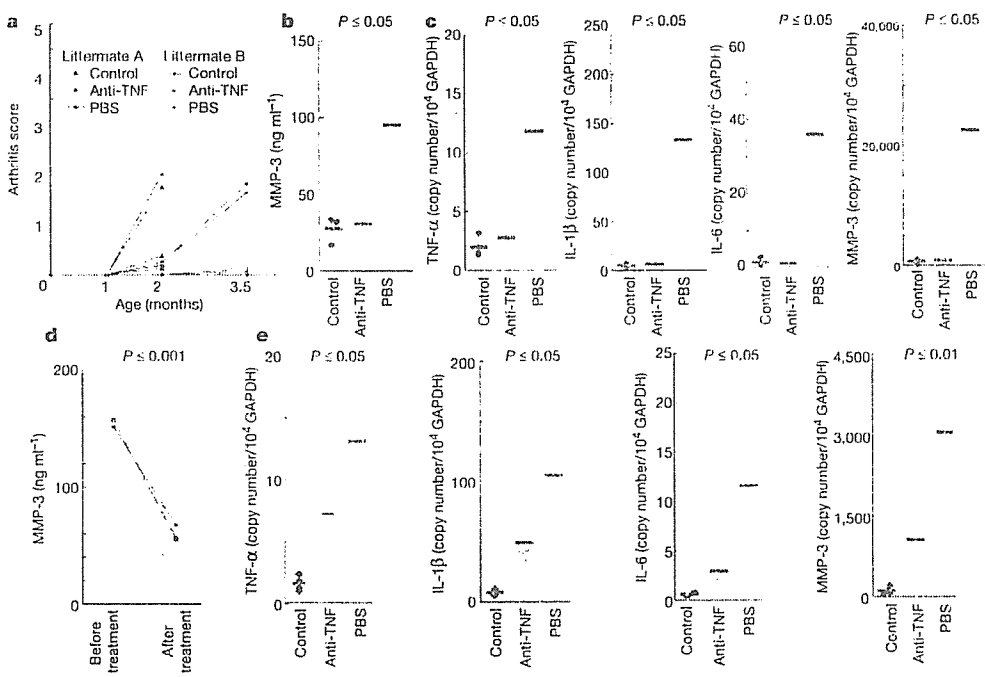

Figure 4 | Protective and therapeutic effect of anti-TNF-α.
a, *DNase II*$^{-/-}$*IFN-IR*$^{-/-}$ (red and blue results) and *DNase II*$^{+/-}$*IFN-IR*$^{-/-}$ (green results) mice were generated from two litters (shown as triangles and circles). At the age of 1 month, *DNase II*$^{-/-}$*IFN-IR*$^{-/-}$ mice received anti-TNF-α (blue) or PBS (red) twice a week. The clinical score of polyarthritis was determined at the indicated ages. **b**, Serum MMP level in 2-month-old *DNase II*$^{+/-}$*IFN-IR*$^{-/-}$ (control), anti-TNF-α-treated or PBS-treated *DNase II*$^{-/-}$*IFN-IR*$^{-/-}$ (four mice each). **c**, Levels of mRNA for TNF-α, IL-1β, IL-6 and MMP-3 in the joints of the forefoot from 2–4-month-old *DNase II*$^{+/-}$*IFN-IR*$^{-/-}$, anti-TNF-α-treated or PBS-treated *DNase II*$^{-/-}$*IFN-IR*$^{-/-}$ mice expressed relative to mRNA for glyceraldehyde-3-phosphate dehydrogenase (GAPDH).
d, **e**, *DNase II*$^{-/-}$*IFN-IR*$^{-/-}$ mice 5–13 months old showing a clinical score of 2.5–6.0 were treated twice a week with anti-TNF-α. **d**, The serum MMP-3 level was determined before and after the 3-week treatment. **e**, Levels of mRNA for TNF-α, IL-1β, IL-6 and MMP-3 in the joints of *DNase II*$^{+/-}$*IFN-IR*$^{-/-}$ (control) and anti-TNF-α-treated or untreated mice were determined after 6 weeks. In **b**, **c** and **e**, horizontal red lines indicate the average values. Welch's *t*-test was used to test for difference, and *P* values are shown.

targeting other pro-inflammatory cytokines, or lymphocytes[21–23]. Whether these treatments are also effective for the polyarthritis in *DNase II*-null mice remains to be studied.

We found DNA in the serum of *DNase II*-deficient mice. Injection of bacterial or mitochondrial DNA into joints induces arthritis, which is mediated by TNF-α produced by macrophages in the joints[24,25]. Immune complexes containing self-DNA activate rheumatoid-arthritis-specific B cells[26]. In these cases, Toll-like receptor 9 (TLR9) is necessary for activating the *TNF-α* gene in macrophages and for producing rheumatoid factor in B cells. In contrast, deletion of the *TLR9* gene had no apparent effect on the development of arthritis in *DNase II*$^{-/-}$ *IRF-1R*$^{+/-}$ mice (K.K. and S.N., unpublished observations), indicating that DNA in the serum might not contribute to the pathogenesis directly. In contrast, we found that macrophages carrying undigested DNA were activated and produced TNF-α. Our results are consistent with the findings that the fetal liver macrophages in *DNase II*$^{-/-}$ mice express IFN-β and TNF-α by a TLR-independent mechanism[14] and that cytosolic DNA activates the innate immunity through a TLR-independent system[27,28]. Further characterization of this TLR-independent pathway is needed to explain the molecular mechanism by which cells sense the DNA that has escaped from degradation and cause autoimmunity.

METHODS

Mice. Mice deficient in the *DNase II* and *IFN-1R* genes were described previously[3]. *E2a Cre* (ref. 29) and *MxI Cre* transgenic mice[30] were from the Jackson Laboratory. MRL *lpr* mice were purchased from Japan SLC. The conditional DNase II targeting mice are described in Supplementary Methods. The anti-TNF α monoclonal antibody (20 μg per g body weight) was administered twice a week by intraperitoneal injection, and clinical parameters were assessed 3 days after the last injection.

Clinical assessment, and histology. Swelling of the forelimb and hindlimb joints was inspected manually and scored as follows: 0, no swelling; 1, mild swelling; 2, severe swelling or deformation of the limb or finger. The scores were summed, and a total score (maximum 8) was given to each mouse. The detailed procedures of MRI, radiography and histological analysis are described in Supplementary Methods.

Enzyme-linked immunosorbent assay (ELISA), real-time PCR and serum DNA. The serum levels of TNF-α, IL-18, rheumatoid factor and MMP-3 were determined with ELISA kits from Beckton Dickinson, MBL, Shibayagi and R&D Systems, respectively. Anti-dsDNA and anti-CCP were measured with a MESACUP DNA-II test kit (MBL) and a DIASTAT anti-CCP ELISA kit (Axis-Shield), except that peroxidase-conjugated goat antibody against mouse immunoglobulin (Cappel) was used as the detection antibody. The procedure for real-time PCR, the primers and the assay method for serum DNA are described in Supplementary Methods.

Received 27 July; accepted 14 September 2006.

1. Nagata, S. DNA degradation in development and programmed cell death. *Annu. Rev. Immunol.* 23, 853–875 (2005).
2. Evans, C. J. & Aguilera, R. J. DNase II: genes, enzymes and function. *Gene* 322, 1–15 (2003).
3. Kawane, K. *et al.* Requirement of DNase II for definitive erythropoiesis in the mouse fetal liver. *Science* 292, 1546–1549 (2001).
4. Kawane, K. *et al.* Impaired thymic development in mouse embryos deficient in apoptotic DNA degradation. *Nature Immunol.* 4, 138–144 (2003).
5. Yoshida, H., Okabe, Y., Kawane, K., Fukuyama, H. & Nagata, S. Lethal anemia caused by interferon-β produced in mouse embryos carrying undigested DNA. *Nature Immunol.* 6, 49–56 (2005).
6. Kuhn, R., Schwenk, F., Aguet, M. & Rajewsky, K. Inducible gene targeting in mice. *Science* 269, 1427–1429 (1995).
7. Feldmann, M., Brennan, F. M. & Maini, R. N. Role of cytokines in rheumatoid arthritis. *Annu. Rev. Immunol.* 14, 397–440 (1996).
8. Firestein, G. S., Alvaro-Gracia, J. M. & Maki, R. Quantitative analysis of cytokine gene expression in rheumatoid arthritis. *J. Immunol.* 144, 3347–3353 (1990).
9. Saxne, T., Palladino, M. A. Jr, Heinegard, D., Talal, N. & Wollheim, F. A. Detection of tumor necrosis factor alpha but not tumor necrosis factor beta in rheumatoid arthritis synovial fluid and serum. *Arthritis Rheum.* 31, 1041–1045 (1988).
10. Manicourt, D. H., Fujimoto, N., Obata, K. & Thonar, E. J. Levels of circulating collagenase, stromelysin-1, and tissue inhibitor of matrix metalloproteinases 1 in patients with rheumatoid arthritis. Relationship to serum levels of antigenic keratan sulfate and systemic parameters of inflammation. *Arthritis Rheum.* 38, 1031–1039 (1995).
11. Schellekens, G. A., de Jong, B. A., van den Hoogen, F. H., van de Putte, L. B. & van Venrooij, W. J. Citrulline is an essential constituent of antigenic determinants recognized by rheumatoid arthritis-specific autoantibodies. *J. Clin. Invest.* 101, 273–281 (1998).
12. Cohen, P. L. & Eisenberg, R. A. *Lpr* and *gld*: single gene models of systemic autoimmunity and lymphoproliferative disease. *Annu. Rev. Immunol.* 9, 243–269 (1991).
13. Krieser, R. J. *et al.* Deoxyribonuclease IIa is required during the phagocytic phase of apoptosis and its loss causes lethality. *Cell Death Differ.* 9, 956–962 (2002).
14. Okabe, Y., Kawane, K., Akira, S., Taniguchi, T. & Nagata, S. Toll-like receptor-independent gene induction program activated by mammalian DNA escaped from apoptotic DNA degradation. *J. Exp. Med.* 202, 1333–1339 (2005).
15. Ramprasad, M. P., Terpstra, V., Kondratenko, N., Quehenberger, O. & Steinberg, D. Cell surface expression of mouse macrosialin and human CD68 and their role as macrophage receptors for oxidized low density lipoprotein. *Proc. Natl Acad. Sci. USA* 93, 14833–14838 (1996).
16. Brennan, F. M. *et al.* Reduction of serum matrix metalloproteinase 1 and matrix metalloproteinase 3 in rheumatoid arthritis patients following anti-tumour necrosis factor-alpha (cA2) therapy. *Br. J. Rheumatol.* 36, 643–650 (1997).
17. Keffer, J. *et al.* Transgenic mice expressing human tumour necrosis factor: a predictive genetic model of arthritis. *EMBO J.* 10, 4025–4031 (1991).
18. Feldmann, M. & Maini, R. N. Anti-TNF alpha therapy of rheumatoid arthritis: what have we learned? *Annu. Rev. Immunol.* 19, 163–196 (2001).
19. Feldmann, M. Development of anti-TNF therapy for rheumatoid arthritis. *Nature Rev. Immunol.* 2, 364–371 (2002).
20. Fujii, T., Shingu, M. & Nobunaga, M. Monocyte activation in early onset rheumatoid arthritis. *Ann. Rheum. Dis.* 49, 397–403 (1990).
21. Edwards, J. C. & Cambridge, G. B-cell targeting in rheumatoid arthritis and other autoimmune diseases. *Nature Rev. Immunol.* 6, 394–403 (2006).
22. Bluestone, J. A., St Clair, L. W. & Turka, L. A. CTLA4Ig: bridging the basic immunology with clinical application. *Immunity* 24, 233–238 (2006).
23. Yokota, S. *et al.* Therapeutic efficacy of humanized recombinant anti-interleukin-6 receptor antibody in children with systemic-onset juvenile idiopathic arthritis. *Arthritis Rheum.* 52, 818–825 (2005).
24. Deng, G. M., Nilsson, I. M., Verdrengh, M., Collins, L. V. & Tarkowski, A. Intra-articularly localized bacterial DNA containing CpG motifs induces arthritis. *Nature Med.* 5, 702–705 (1999).
25. Collins, L. V., Hajizadeh, S., Holme, E., Jonsson, I. M. & Tarkowski, A. Endogenously oxidized mitochondrial DNA induces *in vivo* and *in vitro* inflammatory responses. *J. Leukoc. Biol.* 75, 995–1000 (2004).
26. Leadbetter, E. A. *et al.* Chromatin-IgG complexes activate B cells by dual engagement of IgM and Toll-like receptors. *Nature* 416, 603–607 (2002).
27. Stetson, D. B. & Medzhitov, R. Recognition of cytosolic DNA activates an IRF3-dependent innate immune response. *Immunity* 24, 93–103 (2006).
28. Ishii, K. J. *et al.* A Toll-like receptor-independent antiviral response induced by double-stranded B-form DNA. *Nature Immunol.* 7, 40–48 (2006).
29. Williams-Simons, L. & Westphal, H. HaCre—utility of a general deleter strain. *Transgenic Res.* 8, 53–54 (1999).

Supplementary Information is linked to the online version of the paper at www.nature.com/nature.

Acknowledgements We thank E. Aozasa for pathological analysis of the mice, P. Quartier for critical reading of our manuscript, M. Nishikawa, H. Matsuda, T. Matsuki, A. Seiyama and T. Yanagida for advice and discussion, H. Fukuyama for help at the initial stage of this work, and M. Fuji and M. Harayama for secretarial assistance. This work was supported in part by Grants-in-Aid from the Ministry of Education, Science, Sports, and Culture in Japan.

Author Information Reprints and permissions information is available at www.nature.com/reprints. The authors declare no competing financial interests. Correspondence and requests for materials should be addressed to S.N. (nagata@genetic.med.osaka-u.ac.jp).

E2F decoy oligodeoxynucleotide ameliorates cartilage invasion by infiltrating synovium derived from rheumatoid arthritis

TETSUYA TOMITA[1], YASUO KUNUGIZA[1,2], NARUYA TOMITA[4], HIROSHI TAKANO[1,5], RYUICHI MORISHITA[2], YASUFUMI KANEDA[3] and HIDEKI YOSHIKAWA[1]

[1]Department of Orthopaedics, [2]Divisions of Clinical Gene Therapy, [3]Gene Therapy Science, Osaka University Graduate School of Medicine, 2-2 Yamada-oka, Suita, Osaka 565-0871; [4]Division of Nephrology, Department of Internal Medicine, Kawasaki Medical School, 577 Matsushima, Kurashiki, Okayama 701-0192; [5]Second Department of Oral and Maxillofacial Surgery, Kyushu Dental College, 2-6-1 Manazuru, Kokurakita-ku, Kitakyushu 803-8580, Japan

Received January 13, 2006; Accepted March 4, 2006

Abstract. This study examined the ability of E2F decoy oligodeoxynucleotides (ODN) to inhibit proliferation of synovial fibroblasts derived from patients with rheumatoid arthritis (RA). The effect of E2F decoy ODN on cartilage invasion by RA synovium in a murine model of human RA was also investigated. E2F decoy ODN were introduced into synovial tissue and synovial fibroblasts derived from patients with RA using hemagglutinating virus of Japan (HVJ)-liposomes. The effect of E2F decoy ODN on synovial fibroblast proliferation was evaluated by MTT assay and by RT-PCR for the cell cycle regulatory genes proliferating-cell nuclear antigen (PCNA) and cyclin-dependent kinase 2 (cdk2). Changes in production of inflammatory mediators by RA synovial tissue following transfection with E2F decoy ODN were assessed by ELISA. Human cartilage and RA synovial tissue transfected with E2F decoy ODN were co-transplanted in severe combined immunodeficient (SCID) mice. After 4 weeks, the mice were sacrificed and the implants histologically examined for inhibition of cartilage damage by E2F decoy ODN. E2F decoy ODN resulted in significant inhibition of synovial fibroblast proliferation, corresponding with reduced expression of PCNA and cdk2 mRNA in synovial fibroblasts. The production of interleukin-1ß (IL-1ß), IL-6 and matrix metalloproteinase (MMP)-1 by synovial tissue was also significantly inhibited by the introduction of E2F decoy ODN. Further, in an *in vivo* model, cartilage that was co-implanted with RA synovial tissue transfected with E2F decoy ODN exhibited no invasive and progressive cartilage degradation. These data demonstrate that transfection of E2F decoy ODN prevents cartilage destruction by inhibition of synovial cell proliferation, and suggest that transfection of E2F decoy ODN may provide a useful therapeutic approach for the treatment of joint destruction in arthritis.

Correspondence to: Dr Tetsuya Tomita, Department of Orthopaedics, Osaka University Graduate School of Medicine, 2-2 Yamada-oka, Suita, Osaka 565-0871, Japan
E-mail: tomita@ort.med.osaka-u.ac.jp

Key words: decoy oligodeoxynucleotide, cartilage invasion, synovium, rheumatoid arthritis

Introduction

Rheumatoid arthritis (RA) is characterized by synovial hyperplasia with infiltration of various inflammatory cells resulting in invasion of articular cartilage and bone (1). Synovial fibroblasts are thought to play an important role in the pathogenesis of joint destruction in the arthritic joints. Synovial cells are the major source of proinflammatory cytokines and matrix metalloproteinases (MMP) such as IL-1, IL-6, TNF-α, MMP-1 and MMP-3 (2), and expression is clearly apparent at cartilage-pannus junctions (3). The importance of proliferative activity in RA and its association with production of proinflammatory cytokines has been studied (4-6). Therefore, cell cycle regulators are attractive candidates for therapeutic targets to halt joint destruction in RA.

The transcription factor E2F regulates the expression of multiple cell-cycle regulatory genes that are critical to cell growth and proliferation. In G_0/G_1 phase, E2F forms an inactive complex with the hypophoshorylated retinoblastoma (RB) gene product, cyclin A and cdk2. In this condition, the transcriptional activity sequestered E2F is repressed. Once RB is phosphorylated, E2F is released and becomes free to bind to a specific cis element in the promoter region of cell cycle regulatory genes c-myc, c-myb, cdc2, and cdk2 and proliferating cell nuclear antigen (PCNA), thereby transactivating the expression of these genes (7-10). Cell cycle biology involves a complex interaction of multiple growth factors, their receptors, secondary messengers, oncogenes and transcriptional factors. Therefore, the transcriptional factor E2F provides a good single target for cell cycle blockade.

It has been demonstrated that a synthetic double-stranded oligodeoxynucleotide (ODN) with high affinity for a target transcription factor may be introduced into target cells as a 'decoy' to bind the transcription factor, thereby altering gene transcription (11). We have previously demonstrated inhibition of synovial cell proliferation *in vitro* and amelioration

of joint damage *in vivo* using NFκB decoy ODN (12). To determine the utility of cell cycle inhibition in treating RA, the present study examined the ability of E2F decoy ODN to inhibit synovial proliferation and production of proinflammatory mediators. We also examined the effects of E2F decoy ODN on cartilage invasion by synovial tissue derived from RA patients.

Materials and methods

Patients. Synovial tissues were obtained from five patients with RA who were undergoing synovectomy at Osaka University Hospital and affiliated facilities after receipt of informed consent. All the patients were diagnosed clinically with RA according to the 1987 revised diagnostic criteria of the American College of Rheumatology (13). Normal synovial tissues were obtained from three patients who were seen for trauma and had no evidence of arthritis.

Synovial cell preparation. The synovial specimens were finely minced into small pieces, soaked in an enzyme cocktail solution containing 0.1% type IV collagenase, 0.1% hyaluronidase, and 0.01% DNase (all from Sigma Chemical Co., St. Louis, MO), and incubated for 2 h at 37°C in a shaking water bath. After removal of debris by filtration, the cells thus obtained were suspended in Dulbecco's modified Eagle's medium (DMEM), washed twice, resuspended in DMEM with 10% fetal calf serum (FCS), and seeded in culture dishes. After overnight culture, non-adherent cells were removed, while adherent cells were re-cultured. Third passage synovial cells were used in the experiments.

Cell proliferation assay. Synovial cells were seeded on to uncoated 24-well tissue culture plates (Corning Inc., Corning, NY) at 4000 cells/well. The cells were then incubated in DMEM with 10% FCS for 48 h. After transfection of decoy ODN, the medium was changed to fresh DMEM with 10% FCS. Four days after transfection, an index of cell proliferation was determined by using sulphonated tetrazolium salt, and a 4-[3-(4-iodophenyl)-2-(4-nitrophenyl)-2H-5-tetrazolio]-1,3-benzene disulphonate (WST-1) cell counting kit, which is similar to the 3-(4,5-dimethylthiazol-2-yl)-2,5-diphenyl tetrazolium bromide (MTT) assay (14). This compound produces a highly water-soluble formazan dye, which makes the assay procedure easier to perform.

Synthesis of ODN and selection of sequence targets. The sequences of phosphorothioate double-stranded ODN against the E2F-binding site and of scrambled ODN used in this study were reported previously (15). The phosphorothioate ODN utilized in this study had the following sequences:

E2F decoy ODN: 5'-CTAGATTTCCCGCG-3'
3'-TAAAGGGCGCCTAG-5'

Scramble decoy ODN: 5'-CTAGATTTCGAGCG-3'
3'-TAAAGCTCGCCTAG-5'

The E2F ODN has been shown to bind the E2F transcription factor (11,15-17). Synthetic ODN were washed in 70% ethanol, dried and dissolved in sterile Tris-ethylene diamine tetra acetic acid (EDTA) buffer (10 mM Tris, 1 mM EDTA). The supernatant was purified over a nucleic acid purification-10 (NAP-10) column (Pharmacia LKB Biotechnology, Piscataway, NJ), and the ODN concentration was quantitated by spectrophotometry. Single-strand ODNs were annealed for 2 h while gradually cooling from 80 to 25°C.

Transfection using HVJ-liposome method. Phosphatidylserine, phosphatidylcholine, and cholesterol were mixed in a weight ratio of 1:4.8:2 (12,14,18,19). The lipid mixture (10 mg) was deposited on the sides of flask by removal of tetrahydrofuran in a rotary evaporator. Dried lipid was hydrated in 200 ml of balanced salt solution (BBS; 137 mM NaCl, 5.4 mM KCl, 10 mM Tris-HCl, pH 7.6) containing synthetic double-stranded ODN. Liposomes were prepared by shaking and sonication. Purified HVJ (Z strain) was inactivated by ultraviolet irradiation (110 erg/mm^2/sec) for 3 min just before use. The liposome suspension (0.5 ml, containing 10 mg of lipids) was mixed with HVJ (10,000 haemagglutinating units) in a total volume of 4 ml of BBS. The mixture was incubated at 4°C for 10 min and then for 60 min with gentle shaking at 37°C. Free HVJ was removed from the HVJ-liposomes by sucrose density gradient centrifugation. The top layer of gradient containing purified HVJ-liposomes was collected for use. Synovial tissues were cultured in a serum-free medium 6 h prior to the transfection, then washed 3 times with BBS containing 2 mM $CaCl_2$. The HVJ-liposome complex (15 mM of encapsulated ODN) was added to the synovial tissues for 30 min at 37°C. Finally, fresh medium containing 10% FCS was added to the synovial tissues, which were then incubated in a CO_2 incubator.

Estimation of the transfection efficiency. To examine the localization of the transfected FITC-labeled ODN, cryostat sections of synovium transfected with decoy ODN were prepared for fluorescence microscopy. The sections were stained with Hoechst 33342 (Sigma Chemical Co.) and observed under an ultraviolet laser scanning confocal microscope (PCM 2000; Nikon, Tokyo).

RNA extraction and RT-PCR. Twenty-four hours after transfection of E2F decoy ODN, RNA was extracted from synovial tissues by means of RNAzol (Tel-Test Inc., Friendswood, TX). Expression of PCNA, cdk2, and ß-actin mRNA were measured by RT-PCR as described previously (11). Total RNA (1 μg) prepared from synovial fibroblasts was first treated with RNAse-free DNAse. After treatment for 5 min at 94°C, the samples were subjected to reverse transcription using random hexamer primers (Perkin-Elmer Cetus, Norwalk, CT) and Molony murine leukemia virus reverse transcriptase. The primers for PCNA, cdk2, and ß-actin genes used in this study were: The PCNA 5' primer, 5'-ACTCTGCGC TCCGAAGG-3'; the PCNA 3' primer, 5'-TCTCCA ATTAGGCTAAG-3'. The cdk2 5' primer, 5'-CGCTTC ATGGAGAACTTC-3'; the cdk2 3' primer, 5'-ATGGCA GAAAGCTAGGCC-3'. The ß-actin 5' primer, 5'-TTGTAA CCAACTGGGACGATATGG-3'; the ß-actin 3' primer, 5'-GATCTTGATCTTCATGGTGCT-3'. Aliquots of RNA were amplified simultaneously by PCR (30 cycles) performed

with the step-cycle program set to denature at 94°C for 1 min, anneal at 50°C for 1 min, and extend at 72°C for 2 min. PCR products were electrophoresed on 2% agarose gels stained with ethidium bromide. We observed a linear increase in the amplification of PCR products with increased amounts of RNA up to 1 mg, as well as with increasing PCR cycle number until 30 cycles, suggesting that our results truly reflect differences in mRNA expression of PCNA and cdk2. We used ß-actin as an internal control to standardize the amount of total RNA utilized for RT-PCR. We performed other sets of RT-PCR without RNA samples as negative controls to be certain that there was no artificial amplification.

Gel mobility shift assay. The nuclear extract was prepared from cultured synovial fibroblasts using methods described previously (11,14). In brief, synovial fibroblast pellets were homogenized with a Potte-Elvehjem homogenizer in 4 volumes of ice-cold homogenization buffer [10 mM HEPES pH 7.5, 0.5 M sucrose, 0.5 mM spermidine, 0.15 mM spermin, 5 mM EDTA, 0.25 M ethylene glycol tetra acetic acid (EGTA), 7 mM ß-mercaptoethanol, 1 mM phenylmethylsulphonyl fluoride]. After centrifugation at 12,000 g for 30 min at 4°C, the pellets were lysed and homogenized in a Dounce homogenizer in 1 volume of ice-cold homogenization buffer containing 0.1% NP-40. They were then centrifuged at 12,000 g for 30 min at 4°C and the pelleted nuclei were washed twice with ice-cold buffer containing 0.35 M sucrose. The nuclei were pre-extracted with 1 volume of ice-cold homogenization buffer containing 0.05 M NaCl and 10% glycerol for 15 min at 4°C. The nuclei were then extracted with homogenization buffer containing 0.3 M NaCl and 10% glycerol for 1 h at 4°C, following which the concentration of DNA was adjusted to 1 μg/ml. After the nuclear extract was pelleted at 12,000 g for 30 min at 4°C, the supernatant was brought to 45% $(NH_4)_2SO_4$ and stirred for 30 min at 4°C. The precipitated protein was collected at 17,000 g for 30 min, resuspended in homogenization buffer containing 0.35 M of sucrose, and stored in aliquots at -70°C. E2F ODN probes were labeled at the 3' end by means of a 3' end-labeling kit (Clontech Inc., Palo Alto, CA). After end-labeling, ^{32}P-labeled ODN were purified over a nick column (Pharmacia LKB Biotechnology). Binding reactions (10 μl) including the ^{32}P-labeled probe (0.5-1 ng, 10,000-15,000 c.p.m.), and 1 μg of polydeoxy-inosinic-deoxycytidic acid (Sigma Chemical Co.) were incubated with nuclear extract for 30 min at room temperature and then loaded on to a 5% polyacrylamide gel. The gels were subjected to electrophoresis, dried, and pre-incubated with parallel samples 10 min before the addition of the labeled probe.

Enzyme-linked immunosorbent assay (ELISA) quantifications of cytokine levels in synovial tissue supernatants. After transfection of E2F decoy ODN, synovial tissues (150 mg/well) were incubated in triplicate in supplemented DMEM containing 10% FCS for 48 h at 37°C and 5% CO_2. After 48 h of incubation, the supernatants were collected and centrifuged at 600 g for 10 min and stored -20°C. The assays for human IL-1, IL-6 and MMP-1 levels in the supernatant were performed using the Quantikine human ELISA kit (R&D Systems Inc., Minneapolis, MN) by following the manufacturer's protocol.

Organ culture. The synovial tissue specimen was cut into small pieces, washed 3 times in phosphate-buffered saline (PBS), and its wet weight determined. Synovial tissues were cultured on 24-well plates at 150 mg/well in DMEM (Gibco BRL, Grand Island, NY) supplemented with 10% FCS (Hyclone Laboratories, Logan, UT). Synovial tissues were placed for 6 h prior to the transfection in a serum-free medium, then washed 3 times in BSS containing 2 mM $CaCl_2$. The HVJ-liposome complex (1000 μl) containing 1.3 mg of lipid and 50 μg of encapsulated E2F decoy ODN DNA, and HMG-1 was added to the synovial tissues. The tissues were incubated at 4°C for 5 min and then at 37°C for 30 min. After incubation the medium was changed to fresh medium containing 10% FCS.

Preparation of SCID-HuRAg mice. The previously reported SCID mouse model for human RA (20-23) was evaluated as the model for the treatment study. Six-week-old male SCID mice (CB.17/Icr; Japan Clear, Tokyo, Japan) were used for establishment of SCID-HuRAg model. Normal human articular cartilage with subchondral bone was collected from trauma patients with a femoral neck fracture after informed consent at the time of surgery. The complexes of articular cartilage 4.5-mm diameter and RA synovial tissue (100 mg) transfected with E2F decoy ODN or scramble decoy ODN were co-implanted under the skin of SCID mice. The mice were anesthetized with diethyl ether, according to the guidelines established by the Animal Ethics Committee of Osaka University Medical School. A 1-cm incision was made in the middle of the back, and paravertebral muscle was exteriorized. The back muscle was incised, and RA synovial tissue and normal human cartilage were co-implanted. The entire procedure was performed under sterile conditions.

Specimen evaluation. Forty-five days after implantation, implants were removed, immediately cut off the subchondral bone and then snap-frozen in OCT Tissue Tek. To evaluate the effect of E2F decoy ODN on cartilage invasion by RA synovial tissue, the sections were stained with hematoxylin and eosin, and invasion of the articular cartilage and degradation of perichondrocytic cartilage were evaluated by the following previously reported criteria: Invasion score: 0 = no or minimal invasion, 1 = visible invasion (~ >2 cell depths), 2 = invasion (~ >5 cell depths), 3 = deep invasion (~ >10 cell depths). Cartilage degradation scores: 0 = no degradation, 1 = visible degradation, 2 = degradation, 3 = intensive degradation (24).

Statistical analysis. Results are expressed as means ± standard error of the mean (SEM). Mann-Whitney U test was used to determine significant differences. $p<0.05$ was considered significant. All experiments were carried out at least 3 times.

Results

Transfection of FITC-labeled ODN into cells in the synovial tissue. We first verified that double-stranded ODN tagged with FITC at either the 3' or the 5' end could be introduced efficiently into synovial cell nuclei using the HVJ-liposome method. Synovial tissues were fixed 1 and 7 days after transfection and observed by fluorescence microscopy. One day after transfection without HVJ-liposome, little fluorescence was detected in synovial tissue (Fig. 1C). One day after

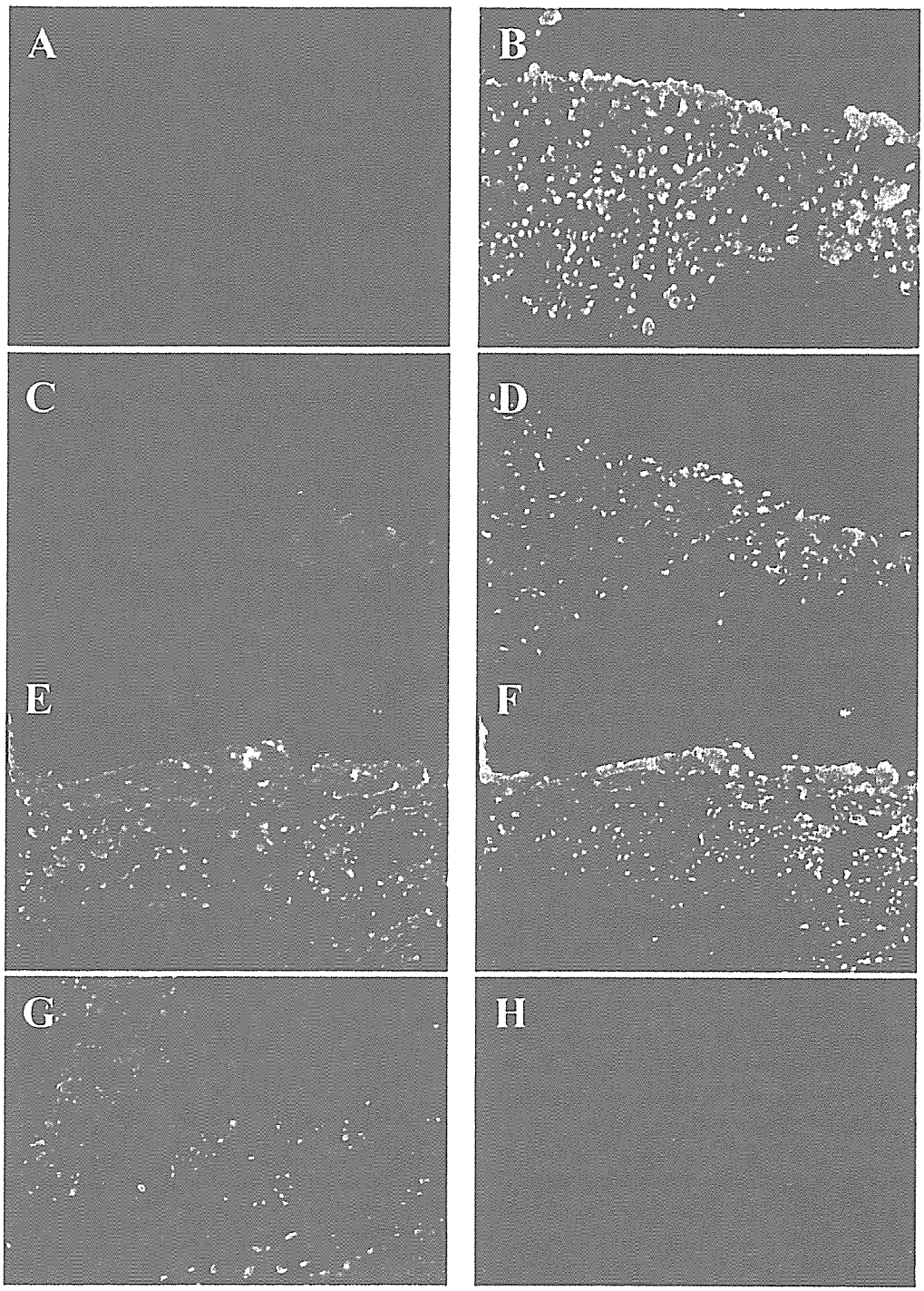

Figure 1 Uptake of FITC-labeled E2F decoy ODN into synovial tissues. Synovial tissues were transfected with FITC-labeled double-stranded ODN (1 μM) with or without the HVJ-liposome method. Synovial tissues were fixed with methanol at 1 and 7 days after transfection, and examined by fluorescence microscopy. (A) Control (transfection with HVJ-liposome method without E2F decoy ODN) (day 1, x100). (C) Direct transfection (1 μM; day 1, x100). (E) Transfection with HVJ-liposome method (1 μM; day 1, x100). (G) Transfection with HVJ-liposome method (1 μM; day 7, x100). (B, D, F and H) The section was counterstained with H&E (B, D and F; day 1, H; day 7, x100).

transfection with the HVJ-liposome method, fluorescence was detected in both the nuclei and the cytoplasm. We detected FITC-labeled ODN in the nuclei of ~50% of the cells (Fig. 1E and F). Even 7 days after transfection with HVJ-liposomes, FITC-labeled ODN were detected in both nuclei and cytoplasm (Fig. 1G and H). No fluorescent signal was seen in the non-transfected cells (Fig. 1 A).

E2F activation in synovial fibroblasts derived from RA. We examined whether or not E2F was suitable target for inhibition of proliferation of synovial fibroblasts derived from RA (Fig. 2). First, we confirmed the upregulation in E2F-binding activity in synovial fibroblasts derived from patients with RA (lane 2). When RA synovial fibroblasts were stimulated with TNF-α, an increase in E2F-binding activity was observed (lane 3). The gel mobility shift assay demonstrated that

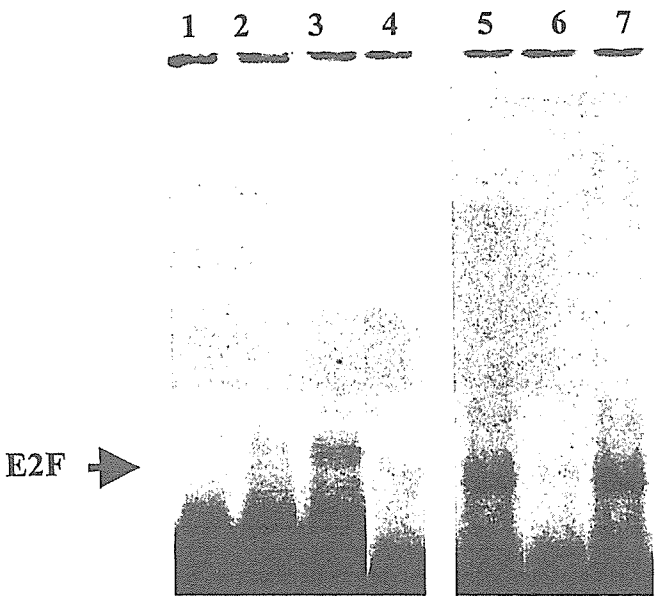

Figure 2. Gel mobility shift assay for E2F activity in nuclear extracts of synovial tissues after decoy transfection. Lane 1, no nuclear extract incubated with a ^{32}P-labeled E2F probe; lanes 2 and 3, nuclear extracts from synovial tissues with RA incubated with a ^{32}P-labeled E2F probe (lane 2, 10 μg; lane 4, 30 μg); lanes 4, nuclear extracts from normal synovial tissues incubated with a ^{32}P-labeled E2F probe (30 μg); lane 5, nuclear extracts from synovial tissues with RA transfected with HVJ-liposome solution alone; lane 6, nuclear extracts from synovial tissues with RA transfected with E2F decoy ODN (10 μM); lane 7, nuclear extracts from synovial tissues with RA transfected with scrambled decoy ODN (10 μM); Detection of E2F in nuclear extracts was specifically inhibited by E2F ODN (lane 6) but not by scrambled ODN (lane 7).

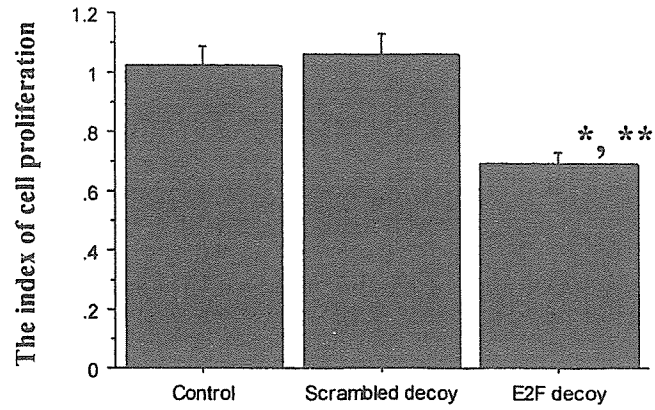

Figure 3. Inhibition of serum-stimulated synovial cells by E2F decoy ODN. The cell count assay using WST-1 was performed 4 days after transfection of decoy ODN. An index of cell proliferation was determined by absorbance at OD 450 nm. The average index of synovial fibroblast cell proliferation (n=5) was expressed as the ratio of control conditions. The result indicated reduced proliferative activity in cells transfected with E2F decoy ODN compared to the cells transfected with scrambled decoy ODN or untreated cells. Each bar represents the mean ± SE. *p<0.01 vs. non-transfected control and **p<0.01 vs. scrambled decoy ODN-treated group.

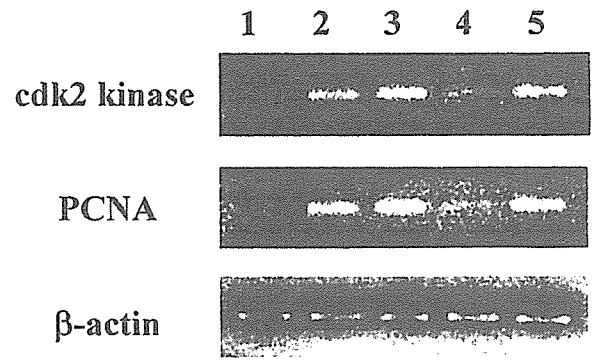

Figure 4. Changes in mRNA expression of cdk2 and PCNA by decoy transfection. Total RNA was extracted from synovial tissues 24 h after transfection with E2F decoy ODN or scrambled decoy ODN, and subjected to RT-PCR analysis for cdk2, PCNA and GAPDH. Lane 1, mRNA from synovial tissues from a trauma patient; lane 2, mRNA from synovial tissues with RA; lane 3, mRNA from synovial tissues with RA after transfection with HVJ-liposome only (without E2F decoy ODN); lane 4, mRNA from synovial tissues with RA after transfection with E2F decoy ODN using HVJ-liposome; lane 5, mRNA from synovial tissue with RA after transfection with scrambled decoy ODN. Total RNA (30 μg) was used for each blot.

E2F-binding activity was enhanced in synovial fibroblasts from patients with RA, but not in synovial fibroblasts from trauma patients (lane 4). This E2F-binding was eliminated by pre-incubation of nuclear extracts with excess amounts of unlabeled E2F ODN. Pre-incubation with excess amounts of unlabeled double-stranded scrambled ODN did not interfere with detection of E2F-binding in TNF-α stimulated synovial fibroblasts derived from RA (lanes 5-7).

Effect of E2F decoy ODN on the inhibition of synovial cell proliferation. One of the characteristic features of RA is abnormal synovial proliferation leading to joint destruction. We investigated the ability of E2F decoy ODN to inhibit synovial cell proliferation. The level of synovial cell proliferation was determined by using the WST-1 cell counting kit 4 days after transfection. The index of cell proliferation determined by absorbance at 450 nm for synovial cells transfected with E2F decoy ODN or with scrambled decoy ODN. Transfection of E2F decoy ODN resulted in a significant inhibition of synovial cell proliferation as compared with scrambled decoy ODN transfected synovial cells and non-transfected synovial cells ($p<0.01$) (Fig. 3).

Effect of E2F decoy ODN on the gene expression of synovial tissues. The transcription factor E2F plays an important role in the transactivation of the cell cycle regulatory genes. We then examined whether or not E2F inhibition would result in decrease of the downstream cell cycle genes such as PCNA and cdk2. Total RNA was extracted from synovial tissues 24 h after transfection with E2F decoy ODN or scrambled decoy ODN, and subjected to RT-PCR analysis for cdk2, PCNA and GAPDH. The expression levels of PCNA and cdk2 gene in untransfected synovial cells were upregulated. Transfection with E2F decoy ODN resulted in a marked attenuation of PCNA and cdk2 gene expression. The 18S rRNA expression level was not affected by E2F decoy ODN (Fig. 4).

Effect of E2F decoy ODN on production of inflammatory cytokines. Since proinflammatory mediators are thought to play a critical role in the pathogenesis of RA, we monitored the production of proinflammatory mediators IL-1ß, IL-6 and MMP-1. The protein levels of IL-1ß, IL-6 and MMP-1 secreted into the culture medium by RA synovial tissue were

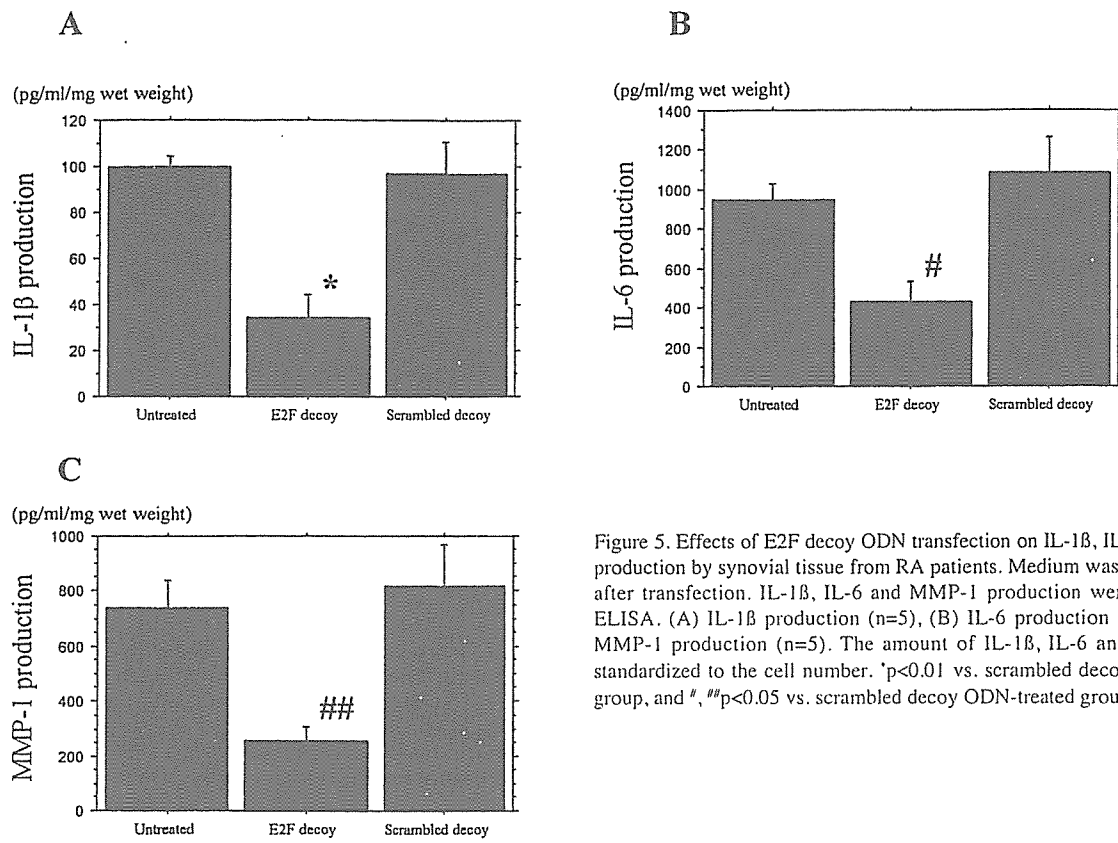

Figure 5. Effects of E2F decoy ODN transfection on IL-1ß, IL-6 and MMP-1 production by synovial tissue from RA patients. Medium was harvested 72 h after transfection. IL-1ß, IL-6 and MMP-1 production were analyzed by ELISA. (A) IL-1ß production (n=5), (B) IL-6 production (n=5) and, (C) MMP-1 production (n=5). The amount of IL-1ß, IL-6 and MMP-1 was standardized to the cell number. *p<0.01 vs. scrambled decoy ODN-treated group, and #, ##p<0.05 vs. scrambled decoy ODN-treated group.

studied 72 h after E2F decoy ODN transfection (n=5 in each group) (Fig. 5). The average level of IL-1ß was 100.2±7.2 pg/ml in untreated group and 104.7±22.5 pg/ml in scrambled decoy group, and 37.4±15.2 pg/ml in E2F decoy group, respectively. The average level of IL-6 was 995±145 pg/ml in untreated group and 1,032±120 pg/ml in scrambled decoy group, and 441±131 pg/ml in E2F decoy group, respectively. The average level of MMP-1 was 775±136 pg/ml in untreated group, 850±372 pg/ml in scrambled decoy group, and 283±76 pg/ml in E2F decoy group, respectively. E2F decoy ODN transfection reduced IL-1ß, IL-6 and MMP-1 production by 54.8±7.4, 42.4±9.5, 28.0±9.9%, respectively. Scrambled decoy ODN had no effect on the production of these mediators.

Marked suppression of invasion of cartilage by RA synovial tissue transfected with E2F decoy ODN. The therapeutic effect of E2F decoy ODN on joint destruction was examined in the severe combined immunodeficient (SCID) mice model for human RA. The volume of RA synovial tissue transfected with E2F decoy ODN was decreased as compared with untreated synovial tissue or synovial tissue transfected with scramble decoy ODN. The articular cartilage co-implanted with RA synovial tissue transfected with scramble decoy ODN showed multiple areas of synovial tissue invasion extending deep into the cartilage. The histological structure of RA synovitis was preserved in these groups. In contrast, the articular cartilage co-implanted with RA synovial tissue transfected with E2F decoy ODN showed marked suppression of invasion by synovial tissue. Infiltrating cells in synovium were decreased in this group (Fig. 6A-F). The grades of cartilage invasion co-implanted with untreated synovial tissue and synovial tissue transfected with scrambled decoy ODN ranged from 1 to 2, with an average of 1.4±0.8 and 1.8±0.4, respectively. The grades of cartilage invasion co-implanted with E2F decoy ODN transfected synovial tissue ranged from 0 to 1, with an average of 0.4±0.5. The grade of cartilage invasion was significantly lower compared with untreated or scrambled decoy ODN group (Fig. 6G).

Discussion

One of the characteristic features of RA is the extensive bone and cartilage erosion caused by the invasive proliferative synovium derived from activated fibroblasts. Thus, cell cycle modulation is an attractive therapeutic target for bone and cartilage erosion in the affected joint of RA. Recent studies demonstrated that suppression of cell cycle in synovial fibroblasts results in inhibition of experimental arthritis (25). Additionally, recent work has found that E2F functions primarily as cell proliferation, suggesting that suppression of transcription of E2F-RB complex suppresses entry into the S phase (26,27). In this study, we used transcription factor E2F decoy oligodeoxynucleotides (ODN) to inhibit synovial cell proliferation. Our data demonstrate that E2F levels in nuclear synovial fibroblast extracts were markedly increased in RA. The specificity of the radiolabeled E2F probe was confirmed by adding a 100-fold excess of unlabeled double stranded E2F decoy ODN to the reaction compared with similar quantities of missense ODN that do not bind E2F. An inhibitory effect of E2F decoy ODN on RA synovial cell proliferation *in vitro* was shown in this study, as well as in the SCID mice model for human RA. Histological examination showed marked reduction of both the volume and cellularity in synovial tissue transfected with E2F decoy ODN. We showed that nuclear E2F expression in RA synovial tissue was downregulated by transfection of E2F decoy ODN following decreased mRNA expression of the

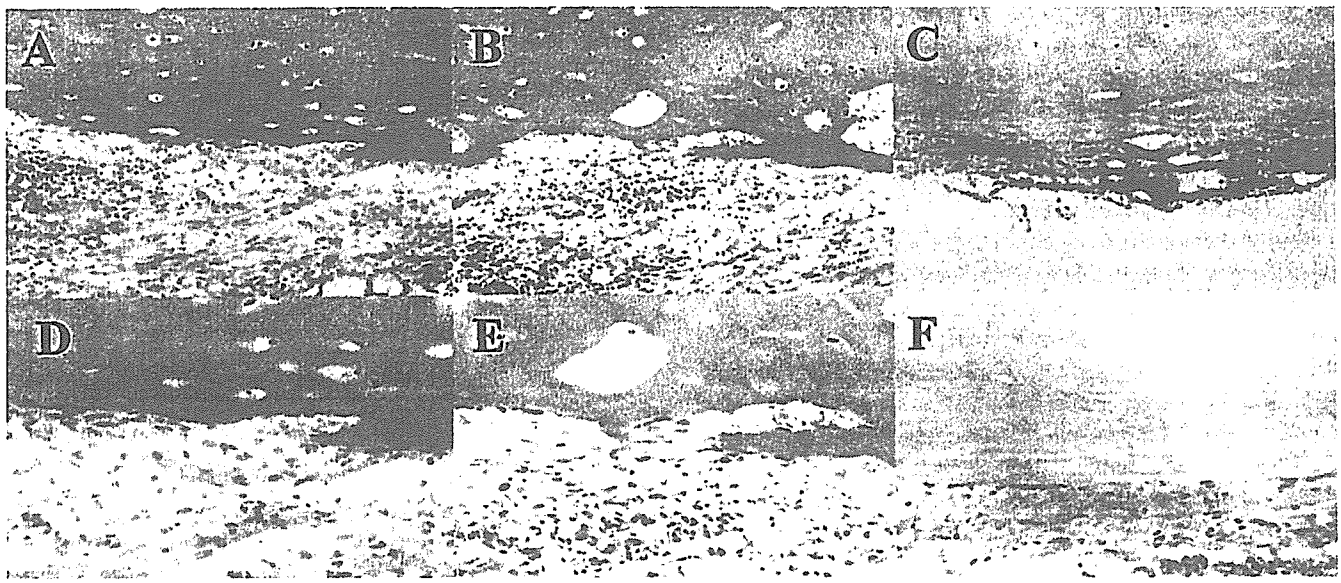

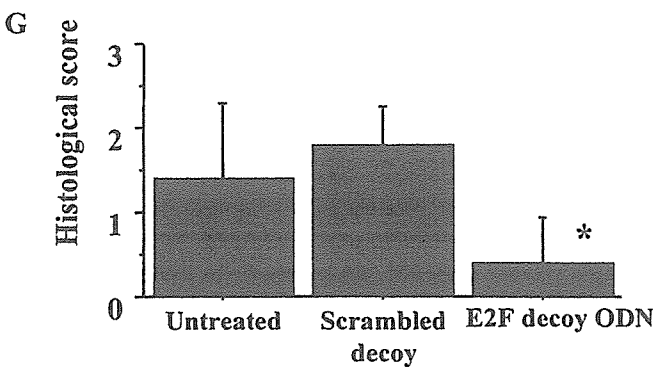

Figure 6. Histological analysis of the co-implanted synovial tissue and cartilage in SCID-HuRAg mice. (A and D) H&E stained sections from untreated synovial tissue. (B and E) H&E stained sections from synovial tissue transfected with scrambled decoy ODN. (C and F) H&E stained sections from synovial tissue transfected with E2F decoy ODN. Untreated synovial tissue and synovial tissue transfected with scrambled decoy ODN showed stratification of synovial cells and infiltration of inflammatory cells. Marked invasion of co-implanted articular cartilage by synovium is apparent (A, B, D and E). Synovial tissue transfected with E2F decoy ODN showed less hyperplasia of synovial cells and infiltration of inflammatory cells. The sections in this group mainly maintained intact cartilage (C and F). (A, B and C; original magnification x200, D, E and F; original magnification x 400). Histological score of the co-implanted synovial tissue and cartilage in SCID-HuRAg mice (n=8 in each group). There was a significant difference in histological score between E2F decoy ODN transfected group and untreated group or scrambled decoy ODN transfected group ($p<0.05$) (G).

cell cycle regulatory genes PCNA and cdk2. These results demonstrated that one mechanism by which E2F decoy ODN reduces synovial cell-associated damage is through inducing cell cycle arrest of synovial cells.

The production of proinflammatory mediators such as IL-1ß, IL-6, and MMP-1 was also suppressed by the transfection of E2F decoy ODN. This might be a secondary effect of inhibition of synovial cell proliferation, as synovial cells are the major producers of proinflammatory mediators in RA. However, the biological significance of E2F decoy ODN on proinflammatory mediator production *in vivo* still remains unclear.

One of the most important strategies for treating RA is prevention of joint destruction. We investigated the inhibitory effect of E2F decoy ODN on cartilage invasion with an *in vivo* murine model for human RA. Human normal articular cartilage and synovial tissue from patients with RA were co-implanted into SCID mice. On the basis of our *in vitro* observations, the predicted effect of E2F inhibition in this model would be prevention of cartilage invasion. The results of this study showed that transfection with E2F decoy ODN significantly suppressed cartilage invasion in this model. The exact etiology and pathogenesis have not yet been fully elucidated; however, stimulation of synovial cells by proinflammatory mediators results not only in proliferation but also in a wide variety of biological responses, including alterations in the generation of many effector molecules potentially involved in the pathological process of cartilage destruction. With respect to this point, E2F decoy ODN strategy would be beneficial not only for inducing cell cycle arrest but also for inhibition of proinflammatory mediator secretion.

New classes of technologies, such as antisense ODN, ribozymes (28-31), and RNA interference (32,33), have been adopted by the arthritis field as strategies to inhibit target gene expression in a sequence-specific manner. In the present study, we used a unique molecular strategy: a synthetic double-stranded DNA with high affinity for a target transcription factor is introduced into target cells as a decoy cis element to bind the transcription factors and alter gene transcription. We previously reported a therapeutic strategy to suppress the inflammatory process in synovial cells by transfecting decoy ODN to block the binding of the critical transcription factor NFκB to its promoter sequence of the target genes, thereby inhibiting the coordinated transactivation of genes of key cytokines and adhesion molecules necessary for the progressive joint destruction in RA (14). Joint destruction was ameliorated by the local injection of NFκB decoy ODN into the affected joints in experimental arthritis models (12). The decoy ODN strategy is more effective than antisense ODN because it blocks multiple transcriptional factors that bind to the same cis element. There are several members of the E2F family, and

this strategy of using an E2F decoy ODN inhibits all E2F members because the decoy competitively blocks binding to the cis element. This ability of decoy ODN to block all transcription factors binding to a particular cis element is the reason that we focused on this technique and we suggest that this method may be more effective than the manipulation of a single cell cycle regulatory gene.

From the therapeutic point of view, the efficiency, stability, and specificity of decoy ODN in the tissue and cellular delivery are the most important issues to address. Specificity of the E2F decoy ODN was clearly shown in this study by gel mobility shift assay. The main limitation of unmodified ODN is the rapid degradation by nucleases prevalent in sera, cell, and tissue. To rectify this problem, ODNs have been chemically modified with sulfur ions, methyl groups, or other modifications to enhance their resistance against nuclease activity. Although the stability of ODNs is enhanced by these chemical modifications, other problems have been encountered that are attributed to foreign materials (28-30). In this study, we employed a circular dumbbell structure (CD) decoy ODN instead of phosphorothioate-modified decoy ODN to overcome the disadvantages of the chemically modified form; so to enhance their uptake and stability in synovial tissue or synovial fibroblast cells, we used the phosphorothioate-modified decoy ODN and HVJ-liposome delivery system. The effectiveness and usefulness of this delivery system has been demonstrated in various disease model both *in vivo* and *in vitro* (35,36). Additional effort is now being applied to use of the circular dumbbell structure decoy ODN instead of phosphorothioate modified decoy ODN to overcome the disadvantages of the chemically modified form (37).

In conclusion, the specificity of the effects of the E2F decoy ODN is supported by the results that only transfection with E2F decoy ODN and not with scrambled decoy ODN could achieve the following effects: a) decreased E2F expression in synovial fibroblasts nuclear extracts, b) decreased mRNA expression of the cell cycle regulatory genes such as cdk2 and PCNA, c) inhibition of cell proliferation, d) decreased production of inflammatory mediators, e) amelioration of cartilage invasion. Since the induction of cell cycle progression appears to be critical for the activation of synovial cells, therapeutic strategies designed to arrest cell cycle progression may prove to be effective in treating cartilage destruction by proliferative synovitis.

Acknowledgements

We wish to thank Drs Hiroaki Matsuno and Tomoatsu Kimura for their excellent technical assistance with animal model experiments. The study was supported in part by grants from the Ministry of Education, Culture, Sport, Science and Technology of Japan, and the Ministry of Health, Labour, and Welfare of Japan.

References

1. Firestein GS: Invasive fibroblast-like synoviocytes in rheumatoid arthritis. Passive responders or transformed aggressors? Arthritis Rheum 39: 1781-1790, 1996.
2. Farahat MN, Yanni G, Poston R and Panayi GS: Cytokine expression in synovial membranes of patients with rheumatoid arthritis and osteoarthritis. Ann Rheum Dis 52: 870-875, 1993.
3. Chu CQ, Field M, Allard S, Abney E, Feldmann M and Maini RN: Detection of cytokines at the cartilage/pannus junction in patients with rheumatoid arthritis: implications for the role of cytokines in cartilage destruction and repair. Br J Rheumatol 31: 653-661, 1992.
4. Michael VV and Alisa KE: Cell cycle implications in the pathogenesis of rheumatoid arthritis. Front Biosci 5: D594-D601, 2000.
5. Nasu K, Kohsaka H, Nonomura Y, Terada Y, Ito H, Hirokawa K and Miyasaka N: Adenoviral transfer of cyclin-dependent kinase inhibitor genes suppresses collagen-induced arthritis in mice. J Immunol 165: 7246-7252, 2000.
6. Perlman H, Bradley K, Liu H, Cole S, Shamiyeh E, Smith RC, Walsh K, Fiore S, Koch AE, Firestein GS, Haines GK 3rd and Pope RM: IL-6 and matrix metalloproteinase-1 are regulated by the cyclin-dependent kinase inhibitor p21 in synovial fibroblasts. J Immunol 170: 838-845, 2003.
7. Dalton S: Cell cycle regulation of the human cdc2 gene. EMBO J 11: 1797-1804, 1992.
8. Thalmeier K, Synovzik H, Mertz R, Winnacker EL and Lipp M: Nuclear factor E2F mediates basic transcription and transactivation by E1a of the human MYC promoter. Genes Dev 3: 527-536, 1989.
9. Wagner S and Green MR: Retinoblastoma. A transcriptional tryst. Nature 352: 189-190, 1991.
10. Watson RJ, Dyson PJ and McMahon J: Multiple c-myb transcript cap sites are variously utilized in cells of mouse haemopoietic origin. EMBO J 6: 1643-1651, 1987.
11. Morishita R, Gibbons GH, Horiuchi M, Ellison KE, Nakama M, Zhang L, *et al*: A gene therapy strategy using a transcription factor decoy of the E2F binding site inhibits smooth muscle proliferation *in vivo*. Proc Natl Acad Sci USA 92: 5855-5859, 1995.
12. Tomita T, Takeuchi E, Tomita N, Morishita R, Kaneko M, Yamamoto K, *et al*: Suppressed severity of collagen-induced arthritis by *in vivo* transfection of nuclear factor kappaB decoy oligodeoxynucleotides as a gene therapy. Arthritis Rheum 42: 2532-2542, 1999.
13. Arnett FC, Edworthy SM, Bloch DA, McShane DJ, Fries JF, Cooper NS, *et al*: The American Rheumatism Association 1987 revised criteria for the classification of rheumatoid arthritis. Arthritis Rheum 31: 315-324, 1988.
14. Tomita T, Takano H, Tomita N, Morishita R, Kaneko M, *et al*: Transcription factor decoy for NFkappaB inhibits cytokine and adhesion molecule expressions in synovial cells derived from rheumatoid arthritis. Rheumatology 39: 749-757, 2000.
15. Tomita N, Horiuchi M, Tomita S, Gibbons GH, Kim JY, Baran D, *et al*: An oligonucleotide decoy for transcription factor E2F inhibits mesangial cell proliferation *in vitro*. Am J Physiol 275: F278-F284, 1998.
16. Mann MJ, Whittemore AD, Donaldson MC, Belkin M, Conte MS, Polak JF, *et al*: *Ex vivo* gene therapy of human vascular bypass grafts with E2F decoy: the PREVENT single-centre, randomised, controlled trial. Lancet 354: 1493-1498, 1999.
17. Ehsan A, Mann MJ, Dell'Acqua G and Dzau VJ: Long-term stabilization of vein graft wall architecture and prolonged resistance to experimental atherosclerosis after E2F decoy oligonucleotide gene therapy. J Thorac Cardiovasc Surg 121: 714-722, 2001.
18. Morishita R, Sugimoto T, Aoki M, Kida I, Moriguchi A, Tomita N, *et al*: *In vivo* transfection of cis element 'decoy' against nuclear factor-kappaB binding site prevents myocardial infarction. Nat Med 3: 894-899, 1997.
19. Kaneda Y, Saeki Y and Morishita R: Gene therapy using HVJ-liposomes: the best of both worlds? Mol Med Today 5: 298-303, 1999.
20. Geiler T, Kriegsmann J, Keyszer GM, Gay RE and Gay S: A new model for rheumatoid arthritis generated by engraftment of rheumatoid synovial tissue and normal human cartilage into SCID mice. Arthritis Rheum 37: 1664-1671, 1994.
21. Müller-Ladner U, Kriegsmann J, Franklin BN, Matsumoto S, Geiler T, Gay RE and Gay S: Synovial fibroblasts of patients with rheumatoid arthritis attach to and invade normal human cartilage when engrafted into SCID mice. Am J Pathol 149: 1607-1615, 1996.
22. Matsuno H, Sawai T, Nezuka T, Uzuki M, Nishimoto N, Tsuji H, and Yoshizaki K: Treatment of rheumatoid synovitis with anti-reshaping human interleukin-6 receptor monoclonal antibody: use of rheumatoid arthritis tissue implants in the SCID mouse model. Arthritis Rheum 41: 2014-2021, 1998.

23. Matsuno H, Yudoh K, Katayama R, Nakazawa F, Uzuki M, Sawai T, Yonezawa T, Saeki Y, Panayi GS, Pitzalis C and Kimura T: The role of TNF-alpha in the pathogenesis of inflammation and joint destruction in rheumatoid arthritis (RA): a study using a human RA/SCID mouse chimera. Rheumatology 41: 329-337, 2002.
24. Müller-Ladner U, Evans CH, Franklin BN, Roberts CR, Gay RE, Robbins PD and Gay S: Gene transfer of cytokine inhibitors into human synovial fibroblasts in the SCID mouse model. Arthritis Rheum 42: 490-497, 1999.
25. Taniguchi K, Kohsaka H, Inoue N, Terada Y, Ito H, Hirokawa K, *et al*: Induction of the p16INK4a senescence gene as a new therapeutic strategy for the treatment of rheumatoid arthritis. Nat Med 5: 760-767, 1999.
26. Murga M, Fernandez-Capetillo O, Field SJ, Borlado LR, Moreno B, Fujiwara Y, *et al*: Mutation of E2F2 in mice causes enhanced T lymphocyte proliferation, leading to the development of autoimmunity. Immunity 15: 959-970, 2001.
27. Harbour JW and Dean DC: Rb function in cell-cycle regulation and apoptosis. Nat Cell Biol 2: E65-E67, 2000.
28. Flory CM, Pavco PA, Jarvis TC, Lesch ME, Wincott FE, Beigelman L, Hunt SW 3rd and Schrier DJ: Nuclease-resistant ribozymes decrease stromelysin mRNA levels in rabbit synovium following exogenous delivery to the knee joint. Proc Natl Acad Sci USA 93: 754-758, 1996.
29. Jarvis TC, Bouhana KS, Lesch ME, Brown SA, Parry TJ, Schrier DJ, Hunt SW 3rd, Pavco PA and Flory CM: Ribozymes as tools for therapeutic target validation in arthritis. J Immunol 165: 493-498, 2000.
30. Takahashi M, Funato T, Suzuki Y, Fujii H, Ishii KK, Kaku M and Sasaki T: Chemically modified ribozyme targeting TNF-alpha mRNA regulates TNF-alpha and IL-6 synthesis in synovial fibroblasts of patients with rheumatoid arthritis. J Clin Immunol 22: 228-236, 2002.
31. Rutkauskaite E, Zacharias W, Schedel J, Muller-Ladner U, Mawrin C, Seemayer CA, Alexander D, Gay RE, Aicher WK, Michel BA, Gay S and Pap T: Ribozymes that inhibit the production of matrix metalloproteinase 1 reduce the invasiveness of rheumatoid arthritis synovial fibroblasts. Arthritis Rheum 50: 1448-1456, 2004.
32. Schedel J, Seemayer CA, Pap T, Neidhart M, Kuchen S, Michel BA, Gay RE, Muller-Ladner U, Gay S and Zacharias W: Targeting cathepsin L (CL) by specific ribozymes decreases CL protein synthesis and cartilage destruction in rheumatoid arthritis. Gene Ther 11: 1040-1047, 2004.
33. Zwicky R, Muntener K, Goldring MB and Baici A: Cathepsin B expression and down-regulation by gene silencing and anti-sense DNA in human chondrocytes. Biochem J 367: 209-217, 2002.
34. Zhou HW, Lou SQ and Zhang K: Recovery of function in osteoarthritic chondrocytes induced by p16INK4a-specific siRNA *in vitro*. Rheumatology 43: 555-568, 2004.
35. Kaneda Y, Yamamoto S and Hiraoka K: The hemagglutinating virus of Japan-liposome method for gene delivery. Methods Enzymol 373: 482-493, 2003.
36. Kaneda Y, Uchida T, Kim J, Ishiura M and Okada Y: The improved efficient method for introducing macromolecules into cells using HVJ (Sendai virus) liposomes with gangliosides. Exp Cell Res 173: 56-69, 1987.
37. Tomita N, Tomita T, Yuyama K, Tougan T, Tajima T, Ogihara T and Morishita R: Development of novel decoy oligonucleotides: advantages of circular dumb-bell decoy. Curr Opin Mol Ther 5: 107-112, 2003.

E2F decoy oligodeoxynucleotide ameliorates cartilage invasion by infiltrating synovium derived from rheumatoid arthritis

TETSUYA TOMITA[1], YASUO KUNUGIZA[1,2], NARUYA TOMITA[4], HIROSHI TAKANO[1,5], RYUICHI MORISHITA[2], YASUFUMI KANEDA[3] and HIDEKI YOSHIKAWA[1]

[1]Department of Orthopaedics, [2]Divisions of Clinical Gene Therapy, [3]Gene Therapy Science, Osaka University Graduate School of Medicine, 2-2 Yamada-oka, Suita, Osaka 565-0871; [4]Division of Nephrology, Department of Internal Medicine, Kawasaki Medical School, 577 Matsushima, Kurashiki, Okayama 701-0192; [5]Second Department of Oral and Maxillofacial Surgery, Kyushu Dental College, 2-6-1 Manazuru, Kokurakita-ku, Kitakyushu 803-8580, Japan

Received January 13, 2006; Accepted March 4, 2006

Abstract. This study examined the ability of E2F decoy oligodeoxynucleotides (ODN) to inhibit proliferation of synovial fibroblasts derived from patients with rheumatoid arthritis (RA). The effect of E2F decoy ODN on cartilage invasion by RA synovium in a murine model of human RA was also investigated. E2F decoy ODN were introduced into synovial tissue and synovial fibroblasts derived from patients with RA using hemagglutinating virus of Japan (HVJ)-liposomes. The effect of E2F decoy ODN on synovial fibroblast proliferation was evaluated by MTT assay and by RT-PCR for the cell cycle regulatory genes proliferating-cell nuclear antigen (PCNA) and cyclin-dependent kinase 2 (cdk2). Changes in production of inflammatory mediators by RA synovial tissue following transfection with E2F decoy ODN were assessed by ELISA. Human cartilage and RA synovial tissue transfected with E2F decoy ODN were co-transplanted in severe combined immunodeficient (SCID) mice. After 4 weeks, the mice were sacrificed and the implants histologically examined for inhibition of cartilage damage by E2F decoy ODN. E2F decoy ODN resulted in significant inhibition of synovial fibroblast proliferation, corresponding with reduced expression of PCNA and cdk2 mRNA in synovial fibroblasts. The production of interleukin-1ß (IL-1ß), IL-6 and matrix metalloproteinase (MMP)-1 by synovial tissue was also significantly inhibited by the introduction of E2F decoy ODN. Further, in an *in vivo* model, cartilage that was co-implanted with RA synovial tissue transfected with E2F decoy ODN exhibited no invasive and progressive cartilage degradation. These data demonstrate that transfection of E2F decoy ODN prevents cartilage destruction by inhibition of synovial cell proliferation, and suggest that transfection of E2F decoy ODN may provide a useful therapeutic approach for the treatment of joint destruction in arthritis.

Correspondence to: Dr Tetsuya Tomita, Department of Orthopaedics, Osaka University Graduate School of Medicine, 2-2 Yamada-oka, Suita, Osaka 565-0871, Japan
E-mail: tomita@ort.med.osaka-u.ac.jp

Key words: decoy oligodeoxynucleotide, cartilage invasion, synovium, rheumatoid arthritis

Introduction

Rheumatoid arthritis (RA) is characterized by synovial hyperplasia with infiltration of various inflammatory cells resulting in invasion of articular cartilage and bone (1). Synovial fibroblasts are thought to play an important role in the pathogenesis of joint destruction in the arthritic joints. Synovial cells are the major source of proinflammatory cytokines and matrix metalloproteinases (MMP) such as IL-1, IL-6, TNF-α, MMP-1 and MMP-3 (2), and expression is clearly apparent at cartilage-pannus junctions (3). The importance of proliferative activity in RA and its association with production of proinflammatory cytokines has been studied (4-6). Therefore, cell cycle regulators are attractive candidates for therapeutic targets to halt joint destruction in RA.

The transcription factor E2F regulates the expression of multiple cell-cycle regulatory genes that are critical to cell growth and proliferation. In G_0/G_1 phase, E2F forms an inactive complex with the hypophoshorylated retinoblastoma (RB) gene product, cyclin A and cdk2. In this condition, the transcriptional activity sequestered E2F is repressed. Once RB is phosphorylated, E2F is released and becomes free to bind to a specific cis element in the promoter region of cell cycle regulatory genes c-myc, c-myb, cdc2, and cdk2 and proliferating cell nuclear antigen (PCNA), thereby trans-activating the expression of these genes (7-10). Cell cycle biology involves a complex interaction of multiple growth factors, their receptors, secondary messengers, oncogenes and transcriptional factors. Therefore, the transcriptional factor E2F provides a good single target for cell cycle blockade.

It has been demonstrated that a synthetic double-stranded oligodeoxynucleotide (ODN) with high affinity for a target transcription factor may be introduced into target cells as a 'decoy' to bind the transcription factor, thereby altering gene transcription (11). We have previously demonstrated inhibition of synovial cell proliferation *in vitro* and amelioration

of joint damage *in vivo* using NFκB decoy ODN (12). To determine the utility of cell cycle inhibition in treating RA, the present study examined the ability of E2F decoy ODN to inhibit synovial proliferation and production of proinflammatory mediators. We also examined the effects of E2F decoy ODN on cartilage invasion by synovial tissue derived from RA patients.

Materials and methods

Patients. Synovial tissues were obtained from five patients with RA who were undergoing synovectomy at Osaka University Hospital and affiliated facilities after receipt of informed consent. All the patients were diagnosed clinically with RA according to the 1987 revised diagnostic criteria of the American College of Rheumatology (13). Normal synovial tissues were obtained from three patients who were seen for trauma and had no evidence of arthritis.

Synovial cell preparation. The synovial specimens were finely minced into small pieces, soaked in an enzyme cocktail solution containing 0.1% type IV collagenase, 0.1% hyaluronidase, and 0.01% DNase (all from Sigma Chemical Co., St. Louis, MO), and incubated for 2 h at 37°C in a shaking water bath. After removal of debris by filtration, the cells thus obtained were suspended in Dulbecco's modified Eagle's medium (DMEM), washed twice, resuspended in DMEM with 10% fetal calf serum (FCS), and seeded in culture dishes. After overnight culture, non-adherent cells were removed, while adherent cells were re-cultured. Third passage synovial cells were used in the experiments.

Cell proliferation assay. Synovial cells were seeded on to uncoated 24-well tissue culture plates (Corning Inc., Corning, NY) at 4000 cells/well. The cells were then incubated in DMEM with 10% FCS for 48 h. After transfection of decoy ODN, the medium was changed to fresh DMEM with 10% FCS. Four days after transfection, an index of cell proliferation was determined by using sulphonated tetrazolium salt, and a 4-[3-(4-iodophenyl)-2-(4-nitrophenyl)-2H-5-tetrazolio]-1,3-benzene disulphonate (WST-1) cell counting kit, which is similar to the 3-(4,5-dimethylthiazol-2-yl)-2,5-diphenyl tetrazolium bromide (MTT) assay (14). This compound produces a highly water-soluble formazan dye, which makes the assay procedure easier to perform.

Synthesis of ODN and selection of sequence targets. The sequences of phosphorothioate double-stranded ODN against the E2F-binding site and of scrambled ODN used in this study were reported previously (15). The phosphorothioate ODN utilized in this study had the following sequences:

E2F decoy ODN: 5'-CTAGATTTCCCGCG-3'
3'-TAAAGGGCGCCTAG-5'

Scramble decoy ODN: 5'-CTAGATTTCGAGCG-3'
3'-TAAAGCTCGCCTAG-5'

The E2F ODN has been shown to bind the E2F transcription factor (11,15-17). Synthetic ODN were washed in 70% ethanol, dried and dissolved in sterile Tris-ethylene diamine tetra acetic acid (EDTA) buffer (10 mM Tris, 1 mM EDTA). The supernatant was purified over a nucleic acid purification-10 (NAP-10) column (Pharmacia LKB Biotechnology, Piscataway, NJ), and the ODN concentration was quantitated by spectrophotometry. Single-strand ODNs were annealed for 2 h while gradually cooling from 80 to 25°C.

Transfection using HVJ-liposome method. Phosphatidylserine, phosphatidylcholine, and cholesterol were mixed in a weight ratio of 1:4.8:2 (12,14,18,19). The lipid mixture (10 mg) was deposited on the sides of flask by removal of tetrahydrofuran in a rotary evaporator. Dried lipid was hydrated in 200 ml of balanced salt solution (BBS; 137 mM NaCl, 5.4 mM KCl, 10 mM Tris-HCl, pH 7.6) containing synthetic double-stranded ODN. Liposomes were prepared by shaking and sonication. Purified HVJ (Z strain) was inactivated by ultraviolet irradiation (110 erg/mm^2/sec) for 3 min just before use. The liposome suspension (0.5 ml, containing 10 mg of lipids) was mixed with HVJ (10,000 haemagglutinating units) in a total volume of 4 ml of BBS. The mixture was incubated at 4°C for 10 min and then for 60 min with gentle shaking at 37°C. Free HVJ was removed from the HVJ-liposomes by sucrose density gradient centrifugation. The top layer of gradient containing purified HVJ-liposomes was collected for use. Synovial tissues were cultured in a serum-free medium 6 h prior to the transfection, then washed 3 times with BBS containing 2 mM $CaCl_2$. The HVJ-liposome complex (15 mM of encapsulated ODN) was added to the synovial tissues for 30 min at 37°C. Finally, fresh medium containing 10% FCS was added to the synovial tissues, which were then incubated in a CO_2 incubator.

Estimation of the transfection efficiency. To examine the localization of the transfected FITC-labeled ODN, cryostat sections of synovium transfected with decoy ODN were prepared for fluorescence microscopy. The sections were stained with Hoechst 33342 (Sigma Chemical Co.) and observed under an ultraviolet laser scanning confocal microscope (PCM 2000; Nikon, Tokyo).

RNA extraction and RT-PCR. Twenty-four hours after transfection of E2F decoy ODN, RNA was extracted from synovial tissues by means of RNAzol (Tel-Test Inc., Friendswood, TX). Expression of PCNA, cdk2, and ß-actin mRNA were measured by RT-PCR as described previously (11). Total RNA (1 μg) prepared from synovial fibroblasts was first treated with RNAse-free DNAse. After treatment for 5 min at 94°C, the samples were subjected to reverse transcription using random hexamer primers (Perkin-Elmer Cetus, Norwalk, CT) and Molony murine leukemia virus reverse transcriptase. The primers for PCNA, cdk2, and ß-actin genes used in this study were: The PCNA 5' primer, 5'-ACTCTGCGC TCCGAAGG-3'; the PCNA 3' primer, 5'-TCTCCA ATTAGGCTAAG-3'. The cdk2 5' primer, 5'-CGCTTC ATGGAGAACTTC-3'; the cdk2 3' primer, 5'-ATGGCA GAAAGCTAGGCC-3'. The ß-actin 5' primer, 5'-TTGTAA CCAACTGGGACGATATGG-3'; the ß-actin 3' primer, 5'-GATCTTGATCTTCATGGTGCT-3'. Aliquots of RNA were amplified simultaneously by PCR (30 cycles) performed

with the step-cycle program set to denature at 94°C for 1 min, anneal at 50°C for 1 min, and extend at 72°C for 2 min. PCR products were electrophoresed on 2% agarose gels stained with ethidium bromide. We observed a linear increase in the amplification of PCR products with increased amounts of RNA up to 1 mg, as well as with increasing PCR cycle number until 30 cycles, suggesting that our results truly reflect differences in mRNA expression of PCNA and cdk2. We used ß-actin as an internal control to standardize the amount of total RNA utilized for RT-PCR. We performed other sets of RT-PCR without RNA samples as negative controls to be certain that there was no artificial amplification.

Gel mobility shift assay. The nuclear extract was prepared from cultured synovial fibroblasts using methods described previously (11,14). In brief, synovial fibroblast pellets were homogenized with a Potte-Elvehjem homogenizer in 4 volumes of ice-cold homogenization buffer [10 mM HEPES pH 7.5, 0.5 M sucrose, 0.5 mM spermidine, 0.15 mM spermin, 5 mM EDTA, 0.25 M ethylene glycol tetra acetic acid (EGTA), 7 mM ß-mercaptoethanol, 1 mM phenylmethylsulphonyl fluoride]. After centrifugation at 12,000 g for 30 min at 4°C, the pellets were lysed and homogenized in a Dounce homogenizer in 1 volume of ice-cold homogenization buffer containing 0.1% NP-40. They were then centrifuged at 12,000 g for 30 min at 4°C and the pelleted nuclei were washed twice with ice-cold buffer containing 0.35 M sucrose. The nuclei were pre-extracted with 1 volume of ice-cold homogenization buffer containing 0.05 M NaCl and 10% glycerol for 15 min at 4°C. The nuclei were then extracted with homogenization buffer containing 0.3 M NaCl and 10% glycerol for 1 h at 4°C, following which the concentration of DNA was adjusted to 1 μg/ml. After the nuclear extract was pelleted at 12,000 g for 30 min at 4°C, the supernatant was brought to 45% $(NH_4)_2SO_4$ and stirred for 30 min at 4°C. The precipitated protein was collected at 17,000 g for 30 min, resuspended in homogenization buffer containing 0.35 M of sucrose, and stored in aliquots at -70°C. E2F ODN probes were labeled at the 3' end by means of a 3' end-labeling kit (Clontech Inc., Palo Alto, CA). After end-labeling, ^{32}P-labeled ODN were purified over a nick column (Pharmacia LKB Biotechnology). Binding reactions (10 μl) including the ^{32}P-labeled probe (0.5-1 ng, 10,000-15,000 c.p.m.), and 1 μg of polydeoxy-inosinic-deoxycytidic acid (Sigma Chemical Co.) were incubated with nuclear extract for 30 min at room temperature and then loaded on to a 5% polyacrylamide gel. The gels were subjected to electrophoresis, dried, and pre-incubated with parallel samples 10 min before the addition of the labeled probe.

Enzyme-linked immunosorbent assay (ELISA) quantifications of cytokine levels in synovial tissue supernatants. After transfection of E2F decoy ODN, synovial tissues (150 mg/well) were incubated in triplicate in supplemented DMEM containing 10% FCS for 48 h at 37°C and 5% CO_2. After 48 h of incubation, the supernatants were collected and centrifuged at 600 g for 10 min and stored -20°C. The assays for human IL-1, IL-6 and MMP-1 levels in the supernatant were performed using the Quantikine human ELISA kit (R&D Systems Inc., Minneapolis, MN) by following the manufacturer's protocol.

Organ culture. The synovial tissue specimen was cut into small pieces, washed 3 times in phosphate-buffered saline (PBS), and its wet weight determined. Synovial tissues were cultured on 24-well plates at 150 mg/well in DMEM (Gibco BRL, Grand Island, NY) supplemented with 10% FCS (Hyclone Laboratories, Logan, UT). Synovial tissues were placed for 6 h prior to the transfection in a serum-free medium, then washed 3 times in BSS containing 2 mM $CaCl_2$. The HVJ-liposome complex (1000 μl) containing 1.3 mg of lipid and 50 μg of encapsulated E2F decoy ODN DNA, and HMG-1 was added to the synovial tissues. The tissues were incubated at 4°C for 5 min and then at 37°C for 30 min. After incubation the medium was changed to fresh medium containing 10% FCS.

Preparation of SCID-HuRAg mice. The previously reported SCID mouse model for human RA (20-23) was evaluated as the model for the treatment study. Six-week-old male SCID mice (CB.17/lcr; Japan Clear, Tokyo, Japan) were used for establishment of SCID-HuRAg model. Normal human articular cartilage with subchondral bone was collected from trauma patients with a femoral neck fracture after informed consent at the time of surgery. The complexes of articular cartilage 4.5-mm diameter and RA synovial tissue (100 mg) transfected with E2F decoy ODN or scramble decoy ODN were co-implanted under the skin of SCID mice. The mice were anesthetized with diethyl ether, according to the guidelines established by the Animal Ethics Committee of Osaka University Medical School. A 1-cm incision was made in the middle of the back, and paravertebral muscle was exteriorized. The back muscle was incised, and RA synovial tissue and normal human cartilage were co-implanted. The entire procedure was performed under sterile conditions.

Specimen evaluation. Forty-five days after implantation, implants were removed, immediately cut off the subchondral bone and then snap-frozen in OCT Tissue Tek. To evaluate the effect of E2F decoy ODN on cartilage invasion by RA synovial tissue, the sections were stained with hematoxylin and eosin, and invasion of the articular cartilage and degradation of perichondrocytic cartilage were evaluated by the following previously reported criteria: Invasion score: 0 = no or minimal invasion, 1 = visible invasion (~ >2 cell depths), 2 = invasion (~ >5 cell depths), 3 = deep invasion (~ >10 cell depths). Cartilage degradation scores: 0 = no degradation, 1 = visible degradation, 2 = degradation, 3 = intensive degradation (24).

Statistical analysis. Results are expressed as means ± standard error of the mean (SEM). Mann-Whitney U test was used to determine significant differences. $p<0.05$ was considered significant. All experiments were carried out at least 3 times.

Results

Transfection of FITC-labeled ODN into cells in the synovial tissue. We first verified that double-stranded ODN tagged with FITC at either the 3' or the 5' end could be introduced efficiently into synovial cell nuclei using the HVJ-liposome method. Synovial tissues were fixed 1 and 7 days after transfection and observed by fluorescence microscopy. One day after transfection without HVJ-liposome, little fluorescence was detected in synovial tissue (Fig. 1C). One day after

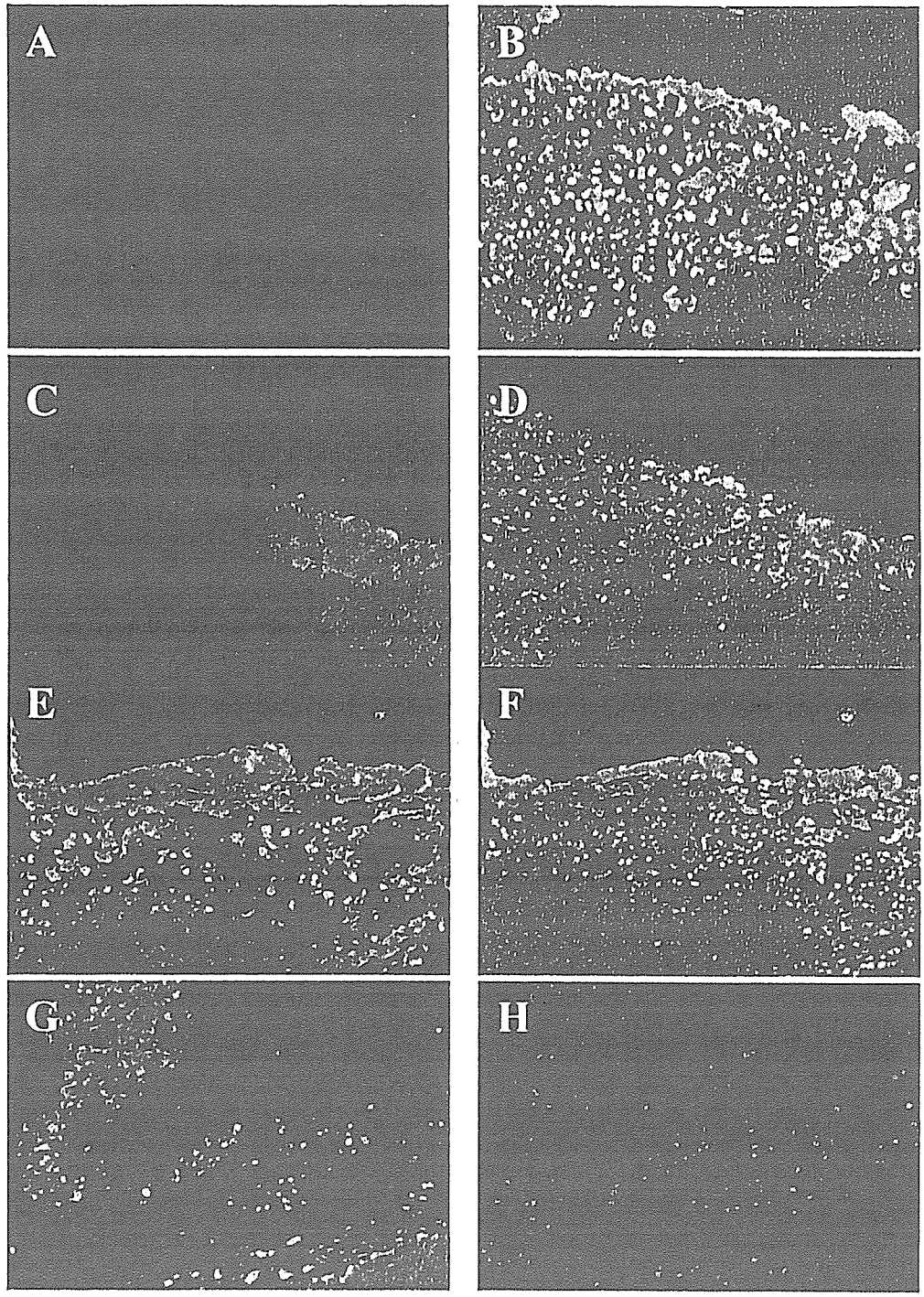

Figure 1 Uptake of FITC-labeled E2F decoy ODN into synovial tissues. Synovial tissues were transfected with FITC-labeled double-stranded ODN (1 μM) with or without the HVJ-liposome method. Synovial tissues were fixed with methanol at 1 and 7 days after transfection, and examined by fluorescence microscopy. (A) Control (transfection with HVJ-liposome method without E2F decoy ODN) (day 1, x100). (C) Direct transfection (1 μM; day 1, x100). (E) Transfection with HVJ-liposome method (1 μM; day 1, x100). (G) Transfection with HVJ-liposome method (1 μM; day 7, x100). (B, D, F and H) The section was counterstained with H&E (B, D and F; day 1, H; day 7, x100).

transfection with the HVJ-liposome method, fluorescence was detected in both the nuclei and the cytoplasm. We detected FITC-labeled ODN in the nuclei of ~50% of the cells (Fig. 1E and F). Even 7 days after transfection with HVJ-liposomes, FITC-labeled ODN were detected in both nuclei and cytoplasm (Fig. 1G and H). No fluorescent signal was seen in the non-transfected cells (Fig. 1 A).

E2F activation in synovial fibroblasts derived from RA. We examined whether or not E2F was suitable target for inhibition of proliferation of synovial fibroblasts derived from RA (Fig. 2). First, we confirmed the upregulation in E2F-binding activity in synovial fibroblasts derived from patients with RA (lane 2). When RA synovial fibroblasts were stimulated with TNF-α, an increase in E2F-binding activity was observed (lane 3). The gel mobility shift assay demonstrated that

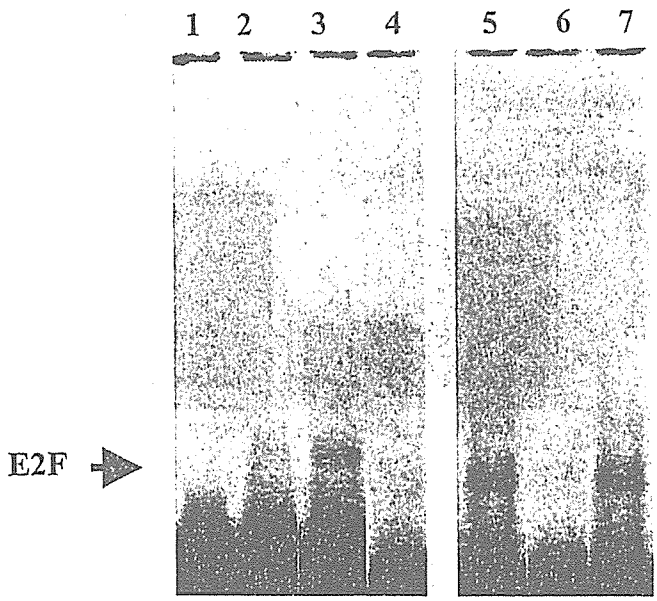

Figure 2. Gel mobility shift assay for E2F activity in nuclear extracts of synovial tissues after decoy transfection. Lane 1, no nuclear extract incubated with a ^{32}P-labeled E2F probe; lanes 2 and 3, nuclear extracts from synovial tissues with RA incubated with a ^{32}P-labeled E2F probe (lane 2, 10 μg; lane 4, 30 μg); lanes 4, nuclear extracts from normal synovial tissues incubated with a ^{32}P-labeled E2F probe (30 μg); lane 5, nuclear extracts from synovial tissues with RA transfected with HVJ-liposome solution alone; lane 6, nuclear extracts from synovial tissues with RA transfected with E2F decoy ODN (10 μM); lane 7, nuclear extracts from synovial tissues with RA transfected with scrambled decoy ODN (10 μM); Detection of E2F in nuclear extracts was specifically inhibited by E2F ODN (lane 6) but not by scrambled ODN (lane 7).

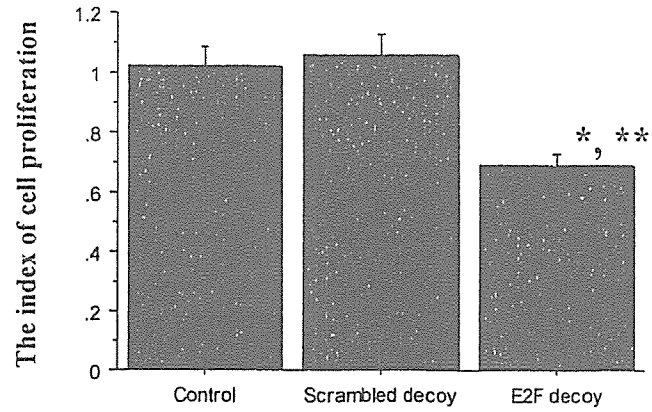

Figure 3. Inhibition of serum-stimulated synovial cells by E2F decoy ODN. The cell count assay using WST-1 was performed 4 days after transfection of decoy ODN. An index of cell proliferation was determined by absorbance at OD 450 nm. The average index of synovial fibroblast cell proliferation (n=5) was expressed as the ratio of control conditions. The result indicated reduced proliferative activity in cells transfected with E2F decoy ODN compared to the cells transfected with scrambled decoy ODN or untreated cells. Each bar represents the mean ± SE. *p<0.01 vs. non-transfected control and **p<0.01 vs. scrambled decoy ODN-treated group.

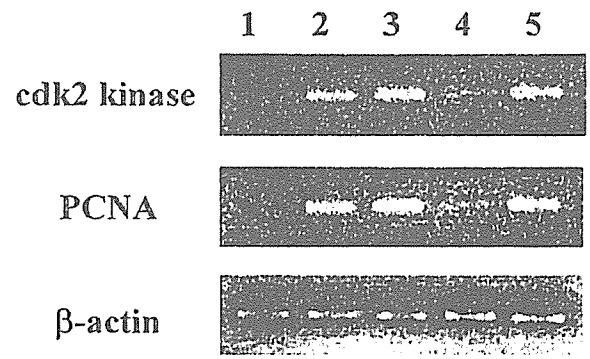

Figure 4. Changes in mRNA expression of cdk2 and PCNA by decoy transfection. Total RNA was extracted from synovial tissues 24 h after transfection with E2F decoy ODN or scrambled decoy ODN, and subjected to RT-PCR analysis for cdk2, PCNA and GAPDH. Lane 1, mRNA from synovial tissues from a trauma patient; lane 2, mRNA from synovial tissues with RA; lane 3, mRNA from synovial tissues with RA after transfection with HVJ-liposome only (without E2F decoy ODN); lane 4, mRNA from synovial tissues with RA after transfection with E2F decoy ODN using HVJ-liposome; lane 5, mRNA from synovial tissue with RA after transfection with scrambled decoy ODN. Total RNA (30 μg) was used for each blot.

E2F-binding activity was enhanced in synovial fibroblasts from patients with RA, but not in synovial fibroblasts from trauma patients (lane 4). This E2F-binding was eliminated by pre-incubation of nuclear extracts with excess amounts of unlabeled E2F ODN. Pre-incubation with excess amounts of unlabeled double-stranded scrambled ODN did not interfere with detection of E2F-binding in TNF-α stimulated synovial fibroblasts derived from RA (lanes 5-7).

Effect of E2F decoy ODN on the inhibition of synovial cell proliferation. One of the characteristic features of RA is abnormal synovial proliferation leading to joint destruction. We investigated the ability of E2F decoy ODN to inhibit synovial cell proliferation. The level of synovial cell proliferation was determined by using the WST-1 cell counting kit 4 days after transfection. The index of cell proliferation determined by absorbance at 450 nm for synovial cells transfected with E2F decoy ODN or with scrambled decoy ODN. Transfection of E2F decoy ODN resulted in a significant inhibition of synovial cell proliferation as compared with scrambled decoy ODN transfected synovial cells and non-transfected synovial cells ($p<0.01$) (Fig. 3).

Effect of E2F decoy ODN on the gene expression of synovial tissues. The transcription factor E2F plays an important role in the transactivation of the cell cycle regulatory genes. We then examined whether or not E2F inhibition would result in decrease of the downstream cell cycle genes such as PCNA and cdk2. Total RNA was extracted from synovial tissues 24 h after transfection with E2F decoy ODN or scrambled decoy ODN, and subjected to RT-PCR analysis for cdk2, PCNA and GAPDH. The expression levels of PCNA and cdk2 gene in untransfected synovial cells were upregulated. Transfection with E2F decoy ODN resulted in a marked attenuation of PCNA and cdk2 gene expression. The 18S rRNA expression level was not affected by E2F decoy ODN (Fig. 4).

Effect of E2F decoy ODN on production of inflammatory cytokines. Since proinflammatory mediators are thought to play a critical role in the pathogenesis of RA, we monitored the production of proinflammatory mediators IL-1ß, IL-6 and MMP-1. The protein levels of IL-1ß, IL-6 and MMP-1 secreted into the culture medium by RA synovial tissue were